

AFAMRL-TR-80-65



**STUDY OF LATERAL EXCESS SOUND
ATTENUATION AS DETERMINED FROM FAR PART
36 AIRCRAFT NOISE CERTIFICATION
MEASUREMENTS**

DWIGHT E. BISHOP

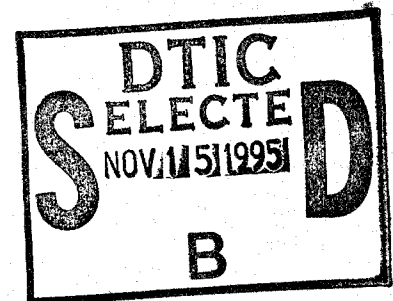
JANE M. BECKMANN

BOLT BERANEK AND NEWMAN INC.

21120 VANOWEN STREET

CANOGA PARK, CALIFORNIA 91303

JULY 1980



19951114 050

Approved for public release; distribution unlimited.

AIR FORCE AEROSPACE MEDICAL RESEARCH LABORATORY
AEROSPACE MEDICAL DIVISION
AIR FORCE SYSTEMS COMMAND
WRIGHT-PATTERSON AIR FORCE BASE, OHIO 45433

DTIC QUALITY INSPECTED 5

NOTICES

When US Government drawings, specifications, or other data are used for any purpose other than a definitely related Government procurement operation, the Government thereby incurs no responsibility nor any obligation whatsoever, and the fact that the Government may have formulated, furnished, or in any way supplied the said drawings, specifications, or other data, is not to be regarded by implication or otherwise, as in any manner licensing the holder or any other person or corporation, or conveying any rights or permission to manufacture, use, or sell any patented invention that may in any way be related thereto.

Please do not request copies of this report from Air Force Aerospace Medical Research Laboratory. Additional copies may be purchased from:

National Technical Information Service
5285 Port Royal Road
Springfield, Virginia 22161

Federal Government agencies and their contractors registered with Defense Documentation Center should direct requests for copies of this report to:

Defense Documentation Center
Cameron Station
Alexandria, Virginia 22314

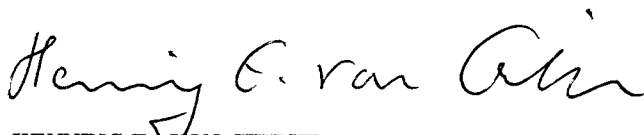
TECHNICAL REVIEW AND APPROVAL

AFAMRL-TR-80-65

This report has been reviewed by the Office of Public Affairs (PA) and is releasable to the National Technical Information Service (NTIS). At NTIS, it will be available to the general public, including foreign nations.

This technical report has been reviewed and is approved for publication.

FOR THE COMMANDER



HENNING E. VON GIERKE
Director
Biodynamics and Bioengineering Division
Air Force Aerospace Medical Research Laboratory

REPORT DOCUMENTATION PAGE		READ INSTRUCTIONS BEFORE COMPLETING FORM
1. REPORT NUMBER AFAMRL-TR-80-65	2. GOVT ACCESSION NO.	3. RECIPIENT'S CATALOG NUMBER
4. TITLE (and Subtitle) STUDY OF LATERAL EXCESS SOUND ATTENUATION AS DETERMINED FROM FAR PART 36 AIRCRAFT NOISE CERTIFICATION MEASUREMENTS		5. TYPE OF REPORT & PERIOD COVERED
		6. PERFORMING ORG. REPORT NUMBER 4225
7. AUTHOR(s) Dwight E. Bishop Jane M. Beckmann		8. CONTRACT OR GRANT NUMBER(s) F 33615-79-C-0501
9. PERFORMING ORGANIZATION NAME AND ADDRESS Bolt Beranek and Newman Inc. 21120 Vanowen Street Canoga Park, CA 91303		10. PROGRAM ELEMENT, PROJECT, TASK AREA & WORK UNIT NUMBERS 62202F 72310709
11. CONTROLLING OFFICE NAME AND ADDRESS Air Force Aerospace Medical Research Laboratory, Aerospace Medical Division, Air Force Systems Command, Wright-Patterson AFB, OH 45433		12. REPORT DATE July 1980
14. MONITORING AGENCY NAME & ADDRESS (if different from Controlling Office)		13. NUMBER OF PAGES 58
		15. SECURITY CLASS. (of this report) Unclassified
		15a. DECLASSIFICATION/DOWNGRADING SCHEDULE
16. DISTRIBUTION STATEMENT (of this Report) Approved for public release; distribution unlimited		
17. DISTRIBUTION STATEMENT (of the abstract entered in Block 20, if different from Report)		
18. SUPPLEMENTARY NOTES		
19. KEY WORDS (Continue on reverse side if necessary and identify by block number) aircraft noise excess attenuation		
20. ABSTRACT (Continue on reverse side if necessary and identify by block number) This report presents information on the variation of the lateral excess attenuation as a function of elevation angle. Lateral excess attenuation represents the differences between the noise levels measured directly underneath the aircraft and to the side of the aircraft, after adjustment for differences in distance and air absorption. This information was developed from analysis of "takeoff" and "sideline" noise data acquired during FAR 36 civil		

aircraft noise certification tests. Curves showing the variation of lateral excess attenuation as a function of elevation angle are shown for individual one-third octave bands from 50 Hz to 2000 Hz and for maximum A-levels and maximum perceived noise levels curves are presented for four aircraft: Lockheed Hercules C-130H, Gates Learjet Model 24D with conical nozzle, Gates Learjet Model 24D with daisy nozzles and shrouds, and Rockwell International Sabreliner NA265-65. Due to differences in the distribution of noise level measurements versus elevation angle among tests, good coverage of elevation angles was obtained only for the C-130H measurements and by combining data for the two Gates Learjet 24D tests.

The study shows that useful excess attenuation information can be developed from aircraft certification data provided steps are taken to locate sideline positions so that measurements adequately cover the range of low elevation angles. The measured excess attenuation values show trends with frequency that are consistent with measurements observed in recent Air Force tests in the frequency range up to about 400 Hz. Larger excess attenuation values were measured at higher frequencies for reasons that are not known at this time. The perceived noise level (PNL), and A-level (AL), curves for each of the aircraft were generally similar in shape however the excess attenuation values for PNL were slightly larger than the AL values, with the difference most pronounced for the C-130H aircraft.

SUMMARY

This report presents information on the variation of the lateral excess attenuation as a function of elevation angle. Lateral excess attenuation represents the differences between the noise levels measured directly underneath the aircraft and to the side of the aircraft, after adjustment for differences in distance and air absorption. This information was developed from analysis of "takeoff" and "sideline" noise data acquired during FAR 36 civil aircraft noise certification tests. Curves showing the variation of lateral excess attenuation as a function of elevation angle are shown for individual one-third octave bands from 50 Hz to 2000 Hz and for maximum A-levels and maximum perceived noise levels curves are presented for four aircraft: Lockheed Hercules C-130H, Gates Learjet Model 24D with conical nozzle, Gates Learjet Model 24D with daisy nozzles and shrouds, and Rockwell International Sabreliner NA265-65. Due to differences in the distribution of noise level measurements versus elevation angle among tests, good coverage of elevation angles was obtained only for the C-130H measurements and by combining data for the two Gates Learjet 24D tests.

The study shows that useful excess attenuation information can be developed from aircraft certification data provided steps are taken to locate sideline positions so that measurements adequately cover the range of low elevation angles. The measured excess attenuation values show trends with frequency that are consistent with measurements observed in recent Air Force tests in the frequency range up to about 400 Hz. Larger excess attenuation values were measured at higher frequencies for reasons that are not known at this time. The perceived noise level (PNL), and A-level (AL), curves for each of the aircraft were generally similar in shape however the excess attenuation values for PNL were slightly larger than the AL values, with the difference most pronounced for the C-130H aircraft.

Accession For	
NTIS GRA&I	<input checked="" type="checkbox"/>
DTIC TAB	<input type="checkbox"/>
Unannounced	<input type="checkbox"/>
Justification	
By	
Distribution/	
Availability Codes	
Dist	Avail and/or Special
A-1	

PREFACE

This research was performed for the Air Force Aerospace Medical Research Laboratory at Wright-Patterson Air Force Base, Ohio under Project/Task 723107, "Technology to Define and Assess Environmental Quality of Noise From Air Force Operations." The guidance of the Technical Monitor for this effort, Mr. Jerry D. Speakman of the Biodynamic Environment Branch, Biodynamics and Bioengineering Division, is gratefully acknowledged.

TABLE OF CONTENTS

	<u>Page</u>
SUMMARY.	1
PREFACE.	2
INTRODUCTION	7
TECHNICAL DISCUSSION	8
General Approach	8
Choice of Noise Spectra for Analysis	8
Major Steps in the Flyover Data Analysis	10
Combining Learjet Model 24D Data	14
PRESENTATION OF DATA	15
DISCUSSION	41
CONCLUSIONS.	48
APPENDIX - EXCESS ATTENUATION CALCULATIONS STEPS AND EQUATIONS.	49
REFERENCES	54

LIST OF ILLUSTRATIONS

<u>Figure</u>		<u>Page</u>
1	TAKEOFF PATH MEASUREMENT GEOMETRY	9
2	GEOMETRY FOR CALCULATION OF "SIDELINE POSITION" DISTANCES AND ANGLES.	12
3	GEOMETRY FOR CALCULATION OF "TAKEOFF POSITION" DISTANCES AND ANGLES.	13
4	EXCESS ATTENUATION RELATIVE TO OVERHEAD MEASUREMENT POSITION - C-130H MEASUREMENTS.	16
5	EXCESS ATTENUATION RELATIVE TO OVERHEAD MEASUREMENT POSITION - LEAR 24 MEASUREMENTS	17
6	EXCESS ATTENUATION RELATIVE TO OVERHEAD MEASUREMENT POSITION - LEAR 24 WITH DAISY NOZZLES MEASUREMENTS.	18
7	EXCESS ATTENUATION RELATIVE TO OVERHEAD MEASUREMENT POSITION - SABRELINER 65 MEASUREMENTS.	19
8-A	EXCESS ATTENUATION RELATIVE TO OVERHEAD MEASUREMENT POSITION IN ONE-THIRD OCTAVE FREQUENCY BANDS - LOCKHEED C-130H	20
8-B	EXCESS ATTENUATION RELATIVE TO OVERHEAD MEASUREMENT POSITION IN ONE-THIRD OCTAVE FREQUENCY BANDS - LOCKHEED C-130H	21
8-C	EXCESS ATTENUATION RELATIVE TO OVERHEAD MEASUREMENT POSITION IN ONE-THIRD OCTAVE FREQUENCY BANDS - LOCKHEED C-130H	22
9-A	EXCESS ATTENUATION RELATIVE TO OVERHEAD MEASUREMENT POSITION IN ONE-THIRD OCTAVE FREQUENCY BANDS - LEARJET 24.	23
9-B	EXCESS ATTENUATION RELATIVE TO OVERHEAD MEASUREMENT POSITION IN ONE-THIRD OCTAVE FREQUENCY BANDS - LEARJET 24.	24
9-C	EXCESS ATTENUATION RELATIVE TO OVERHEAD MEASUREMENT POSITION IN ONE-THIRD OCTAVE FREQUENCY BANDS - LEARJET 24.	25
10-A	EXCESS ATTENUATION RELATIVE TO OVERHEAD MEASUREMENT POSITION IN ONE-THIRD OCTAVE FREQUENCY BANDS - LEARJET 24 WITH DAISY NOZZLES	26

LIST OF ILLUSTRATIONS (CONTINUED)

<u>Figure</u>		<u>Page</u>
10-B	EXCESS ATTENUATION RELATIVE TO OVERHEAD MEASUREMENT POSITION IN ONE-THIRD OCTAVE FREQUENCY BANDS - LEARJET 24 WITH DAISY NOZZLES.27
11-A	EXCESS ATTENUATION RELATIVE TO OVERHEAD MEASUREMENT POSITION IN ONE-THIRD OCTAVE FREQUENCY BANDS - SABRELINER 65.28
11-B	EXCESS ATTENUATION RELATIVE TO OVERHEAD MEASUREMENT POSITION IN ONE-THIRD OCTAVE FREQUENCY BANDS - SABRELINER 65.29
12-A	EXCESS ATTENUATION RELATIVE TO OVERHEAD MEASUREMENT POSITION IN ONE-THIRD OCTAVE FREQUENCY BANDS - COMBINED LEARJET 24 DATA (STANDARD AND DAISY NOZZLES)30
12-B	EXCESS ATTENUATION RELATIVE TO OVERHEAD MEASUREMENT POSITION IN ONE-THIRD OCTAVE FREQUENCY BANDS - COMBINED LEARJET 24 DATA (STANDARD AND DAISY NOZZLES)31
13	EXCESS ATTENUATION IN TERMS OF A-LEVELS AND PERCEIVED NOISE LEVELS - LOCKHEED C-130H32
14	EXCESS ATTENUATION IN TERMS OF A-LEVELS AND PERCEIVED NOISE LEVELS - LEARJET 24.33
15	EXCESS ATTENUATION IN TERMS OF A-LEVELS AND PERCEIVED NOISE LEVELS - LEARJET 24 WITH DAISY NOZZLES.34
16	EXCESS ATTENUATION IN TERMS OF A-LEVELS AND PERCEIVED NOISE LEVELS - SABRELINER 6535
17	EXCESS ATTENUATION IN TERMS OF A-LEVELS AND PERCEIVED NOISE LEVELS - COMBINED LEAR 24 DATA (STANDARD AND DAISY NOZZLES)36
18	COMPARISON OF EXCESS ATTENUATION FOR TWO DEGREE ELEVATION ANGLE.37
19	COMPARISON OF EXCESS ATTENUATION FOR FIVE DEGREE ELEVATION ANGLE.38
20	COMPARISON OF EXCESS ATTENUATION FOR TEN DEGREE ELEVATION ANGLE.39

LIST OF ILLUSTRATIONS (CONTINUED)

<u>Figure</u>		<u>Page</u>
21	COMPARISON OF EXCESS ATTENUATION FOR TWENTY DEGREE ELEVATION ANGLE40
22	AVERAGE NORMALIZED NOISE SPECTRA AT OVERHEAD POSITION (90° ELEVATION ANGLE, 2000 FEET DISTANCE) - LOCKHEED C-130H.42
23	AVERAGE NORMALIZED NOISE SPECTRA AT OVERHEAD POSITION (90° ELEVATION ANGLE, 2000 FEET DISTANCE) - LEARJET 2443
24	AVERAGE NORMALIZED NOISE SPECTRA AT OVERHEAD POSITION (90° ELEVATION ANGLE, 2000 FEET DISTANCE) - LEARJET 24 WITH DAISY NOZZLES.44
25	AVERAGE NORMALIZED NOISE SPECTRA AT OVERHEAD POSITION (90° ELEVATION ANGLE, 2000 FEET DISTANCE) - SABRELINER 65.45

STUDY OF LATERAL EXCESS SOUND ATTENUATION AS DETERMINED FROM FAR
PART 36 AIRCRAFT NOISE CERTIFICATION MEASUREMENTS

INTRODUCTION

At positions to the side of an aircraft flight path, measured noise levels are frequently lower than predicted on the basis of levels observed directly under the flight path, after adjustment for differences in propagation distance and air absorption. This additional attenuation, termed lateral excess attenuation in this report, generally increases in magnitude as the elevation angle (from ground observation point to aircraft) decreases. This lateral excess attenuation is due to several factors, including shielding by the aircraft, scattering during propagation through the atmosphere close to the ground, and attenuation due to propagation at low angles to the surface of the ground.

For accurate prediction of noise levels on the ground to the side of the aircraft flight path during takeoff and landings, information on this lateral excess attenuation as a function of the elevation angle (as seen from the ground observation point) is needed. This report describes the experimental determination of lateral excess sound attenuation based upon analysis of the "takeoff" and "sideline" data acquired during formal FAR 36 certification tests of turboprop and business jet aircraft.

Noise data from fifteen certification tests conducted by BBN were reviewed for completeness of noise and performance data and sideline timing information. The latter was essential for determination of elevation angles at sideline positions. From these tests, seven were selected for detailed study. Of the seven selected, complete analyses were undertaken for four sets of measurements. These are discussed in this report.

The four aircraft selected for analysis were (references 1, 2, 3, 4):

1. Lockheed Hercules C-130H (Lockheed 382E and 382G) equipped with four Allison 501D22 turboprop engines.
2. Gates Learjet Model 24D with two GE CJ-610-6 turbojet engines.
3. Gates Learjet Model 24D with two GE CJ-610-8 turbojet engines with daisy nozzles and shrouds.
4. Rockwell International Sabreliner NA 265-65 with two Airesearch TFE 731-3R-10 turbofan engines.

TECHNICAL DISCUSSION

General Approach

FAR 36 certification takeoff tests involve measurements at a "take-off" position location 3.5 nautical miles from start of takeoff roll, directly under the aircraft flight path, and a number of sideline positions as indicated schematically in Figure 1. For the test data available for review, there were four sideline positions, three on one side and one on the opposite side (not shown in Figure 1). The sideline positions were spaced to cover a wide range of elevation angles.

The general approach in the analysis was to compare the "maximum" one-third octave band levels at several sideline positions with those at the "takeoff" position, after adjustment of the spectra to a constant reference distance, aircraft airspeed and engine thrust for each flight. Perceived noise levels (PNL) and A-levels (AL) were calculated for the adjusted spectra.

Differences in PNL and AL, and one-third octave band levels were then determined as a function of elevation angle. Regression curves were fitted in the data from all flights to obtain sets of curves showing the variation of excess attenuation with angle in one-third octave bands, and in terms of PNL and AL values.

The major advantages of using already-acquired certification data are that:

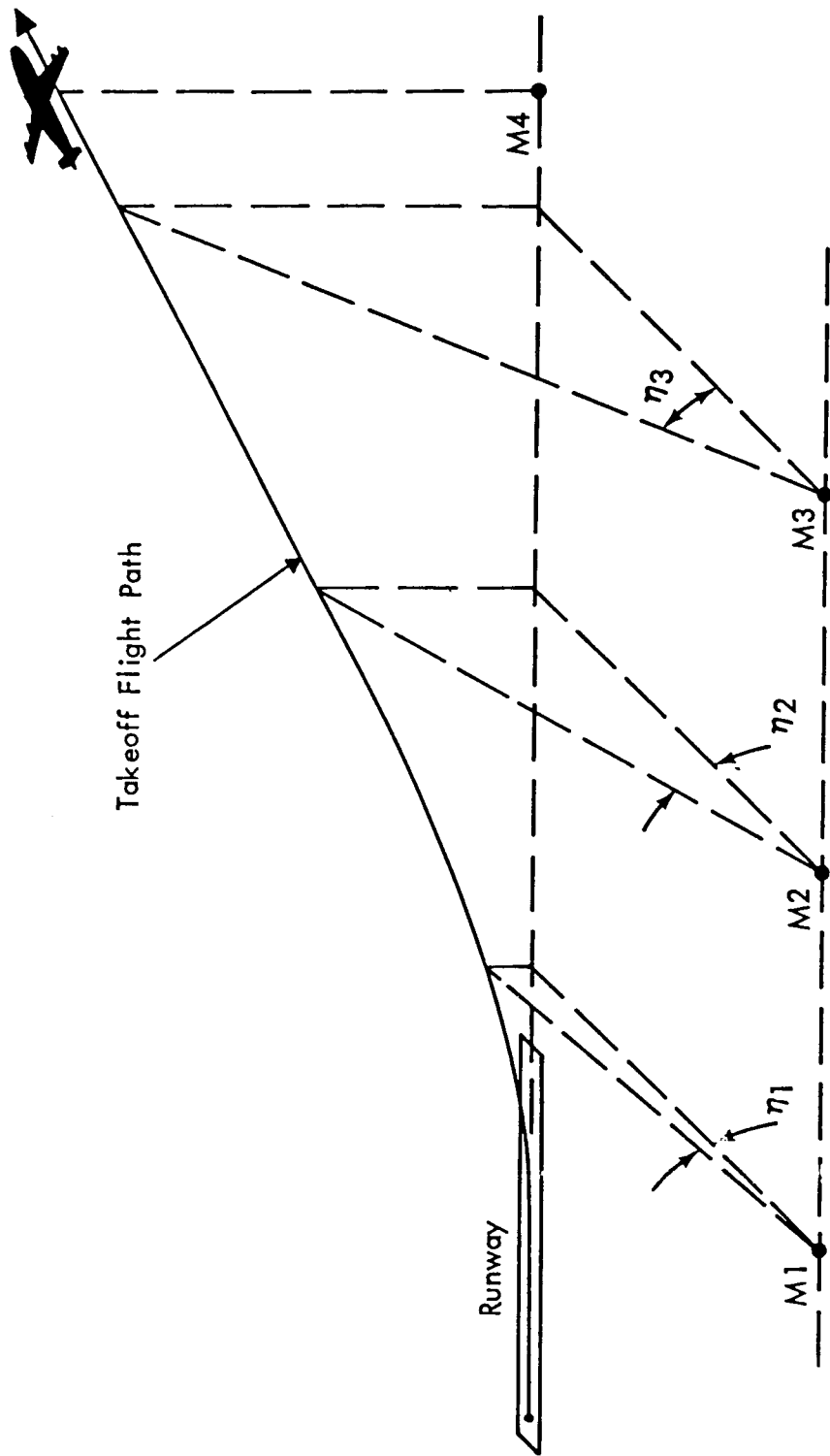
- (a) Noise and aircraft performance data have been acquired under carefully documented conditions.
- (b) The noise data have already been reduced to sets of one-third octave band spectra at half second intervals.
- (c) Data from repeat flights are available.

The major disadvantages of the available certification data are:

- (a) The sideline locations, typically three in number for the tests available for this project, do not necessarily cover the range of small elevation angles of most interest.
- (b) The accuracy of timing information for some of the sideline data available from earlier certification tests did not allow accurate calculation of some of the adjustments to reference conditions.

Choice of Noise Spectra for Analysis

Two sets of "maximum" type spectra were employed in the analysis.



η - Elevation Angle
 M - Microphone

FIGURE 1. TAKEOFF PATH MEASUREMENT GEOMETRY

- (a) The composite flyover noise spectrum. The composite spectrum comprises the maximum one-third octave band levels recorded during the flyover event even though these maxima may not have occurred at the same instant in time. (This spectrum may be A-weighted to give a composite A-level which will generally be between zero and 2 dB above the maximum A-level actually recorded during the flyover event.)
- (b) The integrated flyover noise spectrum. The integrated spectrum comprises the time integral of each one-third band during the flyover event normalized to a reference duration of one second. Integration limits for each band were, at a minimum, the 10 dB downpoint during the event. Thus:

$$IL(i) = 10 \log \int_{-\infty}^{+\infty} 10 \frac{L(i)}{10} dt$$

where $IL(i)$ = integrated level of i th frequency band
 $L(i)$ = level of i th frequency band at time t

or, when computed from flyover signals sampled at discrete intervals

$$IL(i) = 10 \log \sum_{K=0}^d 10 \frac{L(i)K}{10} + 10 \log \Delta t$$

where d is the time interval during which $L(i)$ is within 10 dB of the maximum value of $L(i)$, and Δt is the time interval between noise level samples.

The integrated spectrum may also be A-weighted to give a form of the sound exposure level (SEL). Although strictly speaking SEL is a time integral of the A-level time history, in practice the results indicate essentially no numerical difference between the two methods of calculations.

Major Steps in the Flyover Data Analysis

Each major step in determining the excess attenuation for the sideline and takeoff data is listed below. The appendix tabulates each calculation step and provides the working equations for the analysis.

1. Obtain the one-third octave band spectra for each aircraft flight at the sideline and takeoff positions in terms of
 - (a) the composite flyover spectrum

- (b) the integrated flyover spectrum*
2. Determine the following information for each flight**
 - (a) Field temperature and relative humidity.
 - (b) Slant distance at time of closest approach.
 - (c) The angle of radiation (θ) from the aircraft at the time the maximum A-level was generated.
 - (d) Flight speed and thrust at the time of the maximum noise level.
 3. Establish reference slant distance, speed and thrust conditions for all runs.
 4. Adjust both the composite and integrated noise spectra for air absorption taking into account field and reference temperatures and humidities, and field and reference slant distances.
 5. Adjust the composite spectrum levels to reference conditions, adjusting for distance and thrust.
 6. Adjust the integrated spectrum levels to reference conditions, adjusting for distance, thrust and airspeed.
 7. Determine and apply the relative "duration" adjustments for the integrated spectrum levels (i.e., the adjusted difference between maximum and integrated level, determined for each frequency band).

Notes:

- (a) This "duration" adjustment is calculated separately for each frequency band and for PNL and AL data as well, from linear regression lines fitted to the differences between integrated levels and maximum levels plotted versus log (distance), using data from all flights.
- (b) The above steps result in composite and integrated spectrum levels adjusted to reference conditions. Thus in the

* In the analysis, the "10 dB down" duration time was measured for each one-third octave band, and compared with the duration of the recorded tape signal. Levels of frequency bands where the "10 dB down" time was equal to the recorded signal duration were discarded because of insufficient signal-to-noise ratios.

**See Figures 2 and 3 for the basic geometry and identification of angles and distances.

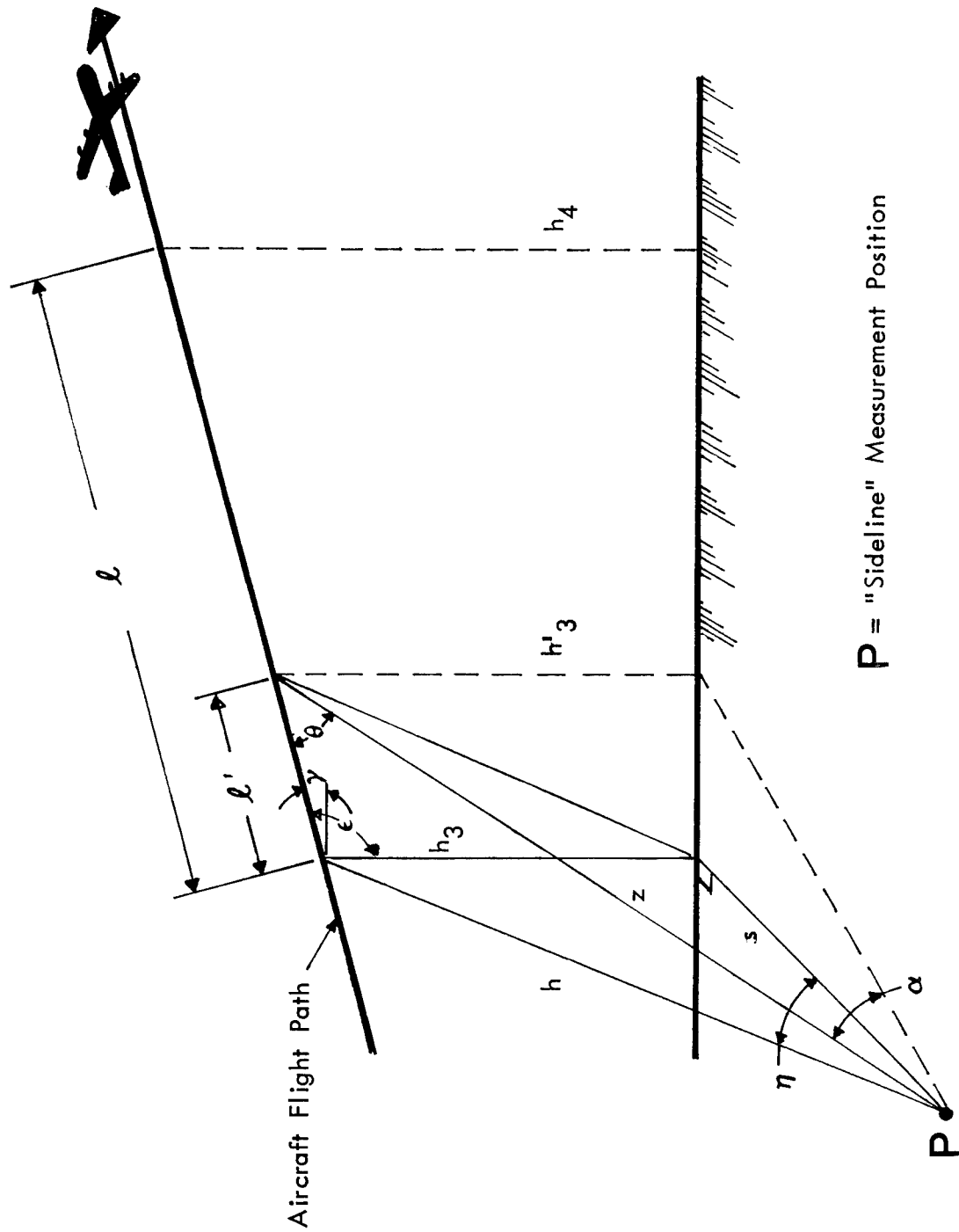


FIGURE 2. GEOMETRY FOR CALCULATION OF "SIDELINE POSITION" DISTANCES AND ANGLES

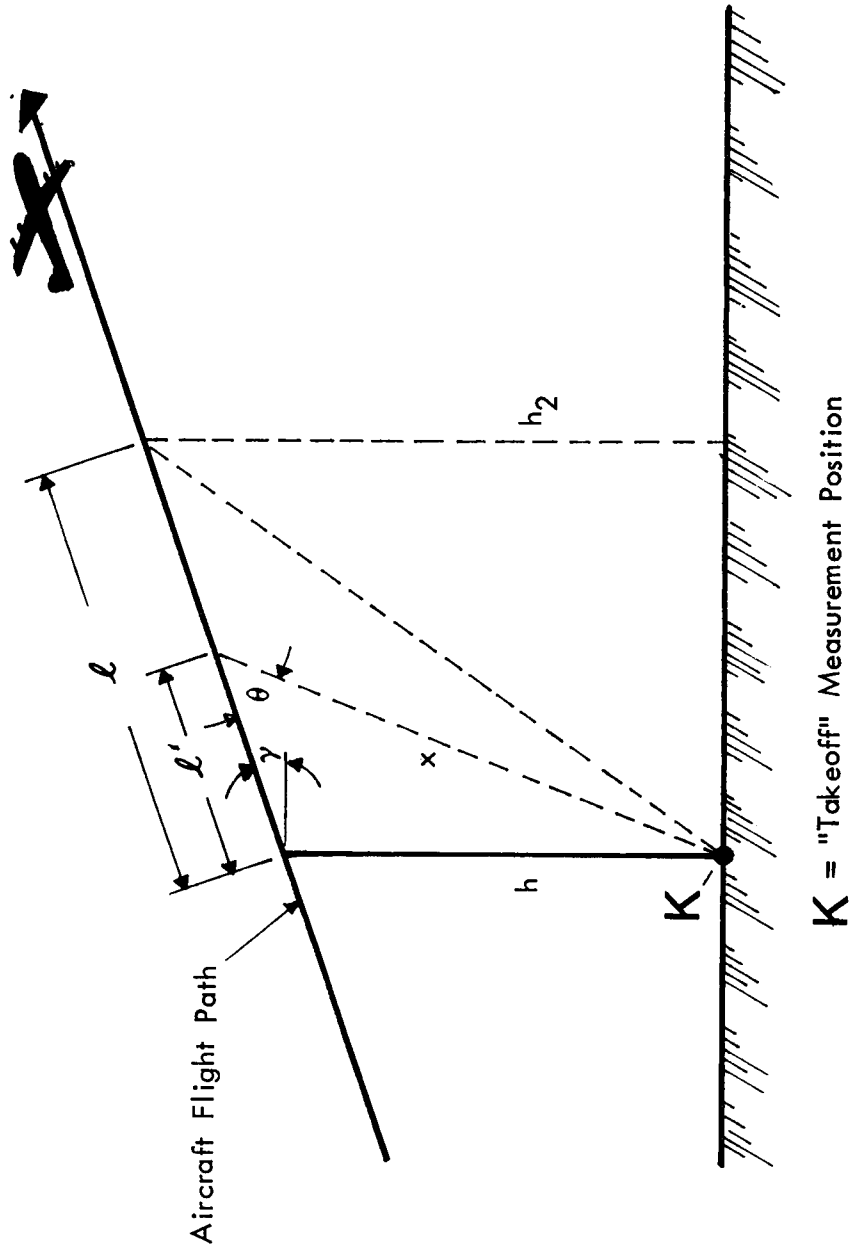


FIGURE 3. GEOMETRY FOR CALCULATION OF "TAKEOFF POSITION" DISTANCES AND ANGLES

following steps, differences in levels, aside from differences arising from experimental error, are assumed to be due to changes in the elevation angles.

8. Calculate the perceived noise level (PNL) and A-level (AL) values for each adjusted spectra.
9. For each flight, determine the differences in each one-third octave band, and for the PNL and AL values between sideline and the overhead (takeoff) position. Tabulate these data as a function of run and position. Note that two sets of differences are obtained for each run: one set for the composite spectrum and another set for the integrated spectrum.
10. Consider these differences as a function of either the sine of η or the logarithm of η , and fit a three-degree polynomial regression curve to the data.*
11. Plot and/or tabulate the differences obtained from the regression curves as a function of angle η .

Combining Learjet Model 24D Data

Two separate sets of certification data were available for the Learjet 24D, with the only difference in airplane configuration being the installation of daisy noise suppressors and shrouds for one set of tests. Because each set of data covered a range of excess elevation angles not measured in the other set (see "Presentation of Data" section), the excess attenuation differences obtained in each one-third octave band (from Step 9) for each set of data were combined. Regression curves were then fitted to the combined data in accord with Step 10.

This approach assumes that the excess attenuation, as determined in one-third octave frequency bands, was unchanged between tests. There was no change in the basic aircraft geometry (the same aircraft was used in both tests), and it was expected that changes in the engine noise characteristics (frequency spectrum and directivity pattern) between tests would produce little change in the measured one-third octave band excess attenuation.

To obtain excess attenuation values in terms of PNL and AL for the combined data, the excess attenuation in one-third octave bands, as obtained from the regression curves, was tabulated for various elevation angles. These values were then applied to the average noise spectrum measured overhead at the takeoff position for each aircraft.** Perceived noise levels and A-levels were then calculated for these adjusted spectra. The PNL and AL values at the different

* The statistical program of Reference 5 was used.

**The spectrum used was the average of the composite spectra obtained from all flights of each aircraft.

elevation angles were then compared with the PNL and A-level for the overhead spectrum to determine the variation in PNL and AL as a function of elevation angle.

This procedure results in a set of PNL and AL excess attenuation curves for each aircraft test, since the overhead spectra for the two aircraft tests differed.

PRESENTATION OF DATA

Results of the analysis of data for the four aircraft are depicted in the series of figures, Figures 4 through 25. Figures 4 through 7 show the calculated excess attenuation versus angle for each flight of each of the four aircraft, for three one-third octave bands--250, 500 and 1000 Hz. Excess attenuation values obtained from the composite (maximum) spectra and from the integrated spectra are coded separately. The plots of the individual data points illustrate the typical variability in data, and the range of elevation angles over which excess attenuation values were calculated. Each figure also showed the calculated regression curve based upon a three degree polynomial in $\sin \eta$.

Figures 8 through 12 show the excess attenuation curves calculated for each one-third octave band from 50 Hz to 2000 Hz (or 5000 Hz for the C-130H).

Figures 8 through 11 show curves for each of the four aircraft, as calculated from each set of certification data. Figure 12 shows the excess attenuation curves for the combined data from the two Learjet 24 tests.

Figures 13 through 17 show the calculated excess attenuation as a function of A-level (AL) and perceived noise level (PNL) for each aircraft. In Figures 13 through 16, two curves are shown for the PNL and AL functions. One curve assumes a three degree polynomial in terms of $\sin \eta$, the other curve assumes a three degree polynomial as a function of $\log \eta$.

Figure 17 shows the excess attenuation for the Lear 24 with standard nozzles and with daisy nozzles, based on the combined excess attenuation data for the two tests. The curves in Figure 17 differ for the two aircraft because the single set of one-third octave band excess attenuation values (Figure 11) has been applied to different overhead spectra (shown later in Figures 23 and 24).

Figures 18 through 21 show the excess attenuation as a function of frequency for selected angles - two degrees, five degrees, 10 degrees, and 20 degrees. These values are based upon the regression curves shown in Figures 8 through 12. Spectra are shown only where field measurements extended to or near the particular elevation angle. Each figure also shows a curve which is an average reported

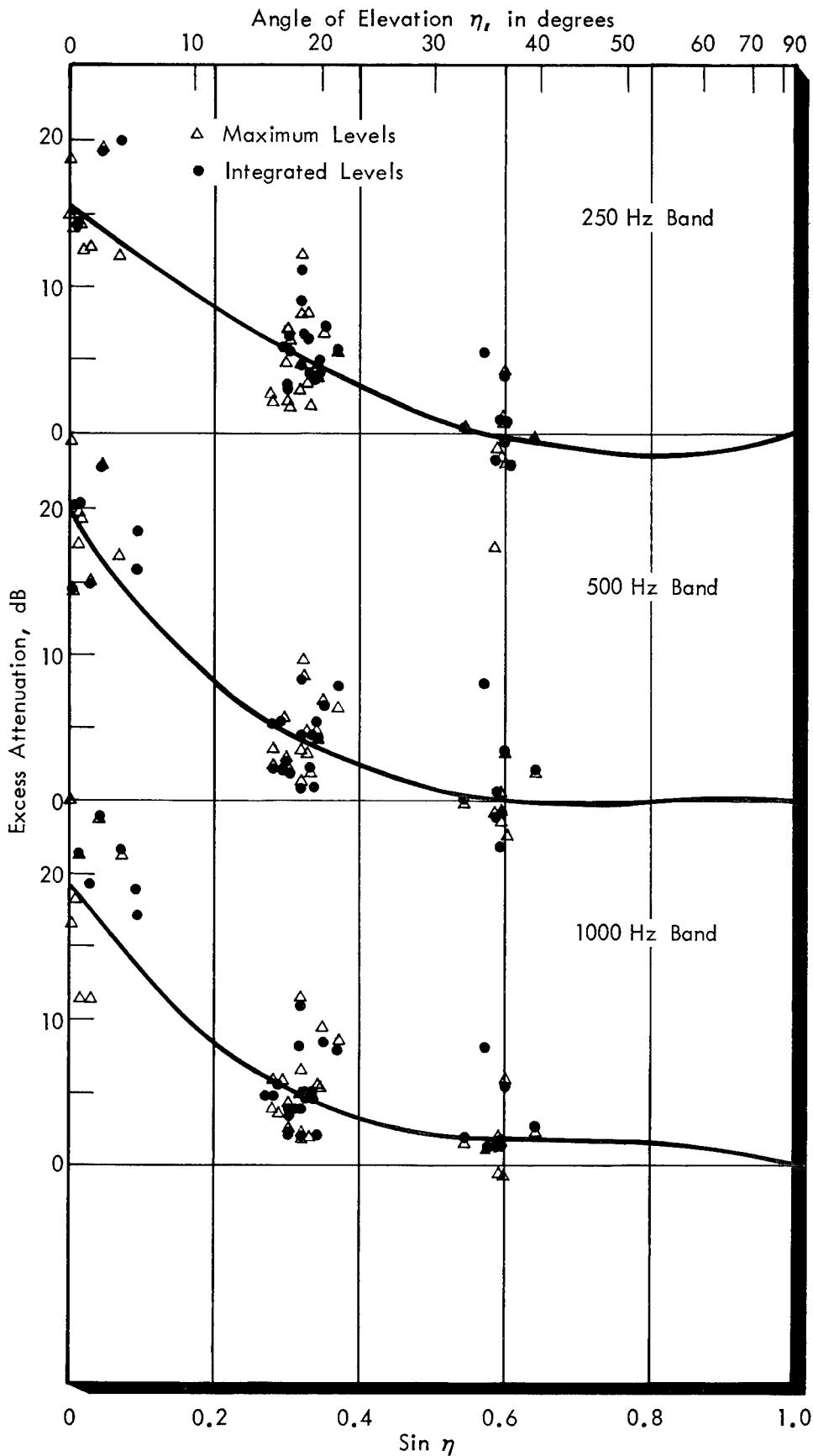


FIGURE 4. EXCESS ATTENUATION RELATIVE TO OVERHEAD MEASUREMENT POSITION - C130H MEASUREMENTS

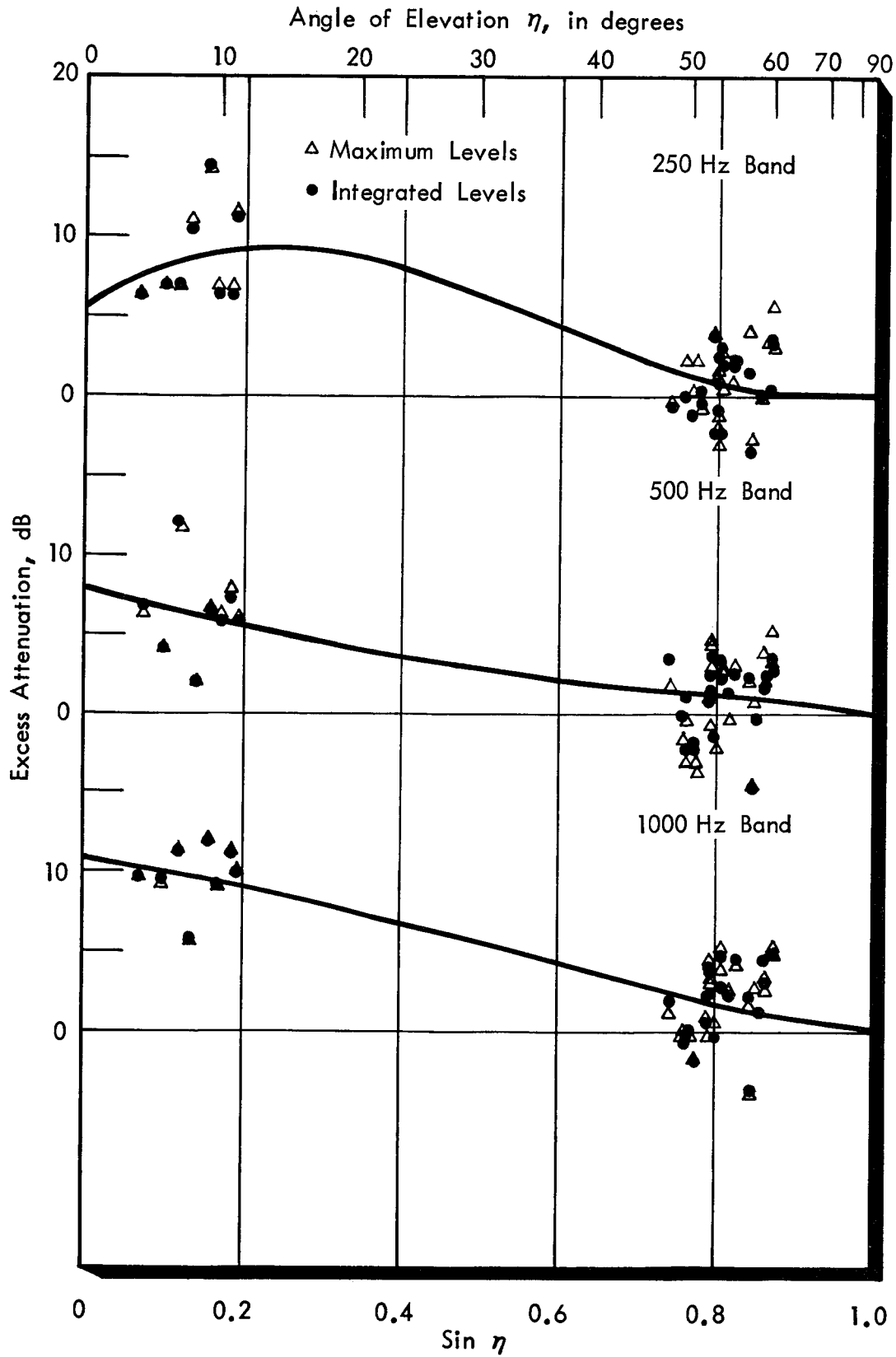


FIGURE 5. EXCESS ATTENUATION RELATIVE TO OVERHEAD MEASUREMENT POSITION - LEAR 24 MEASUREMENTS

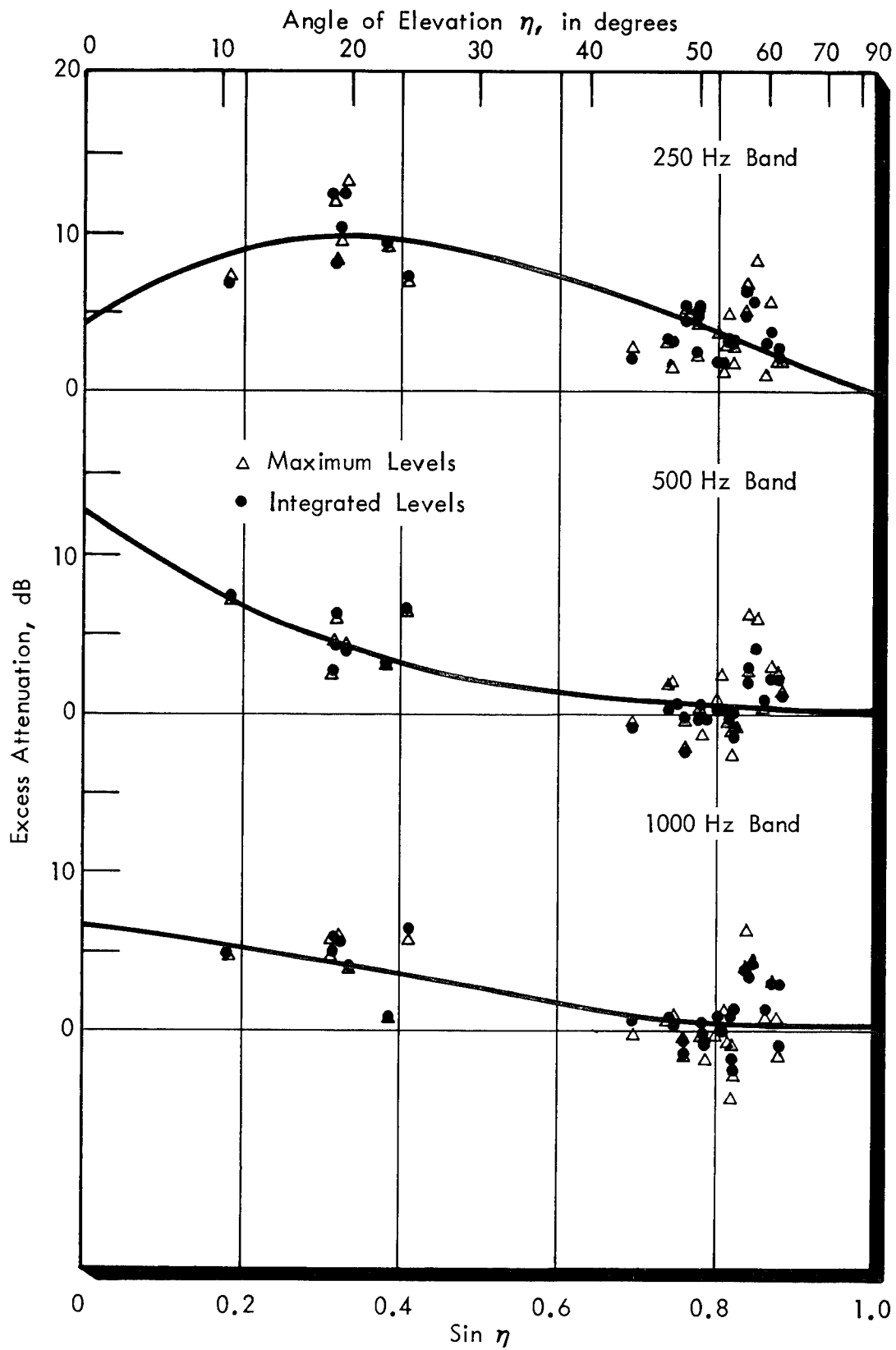


FIGURE 6. EXCESS ATTENUATION RELATIVE TO OVERHEAD MEASUREMENT POSITION - LEAR 24 WITH DAISY NOZZLES MEASUREMENTS

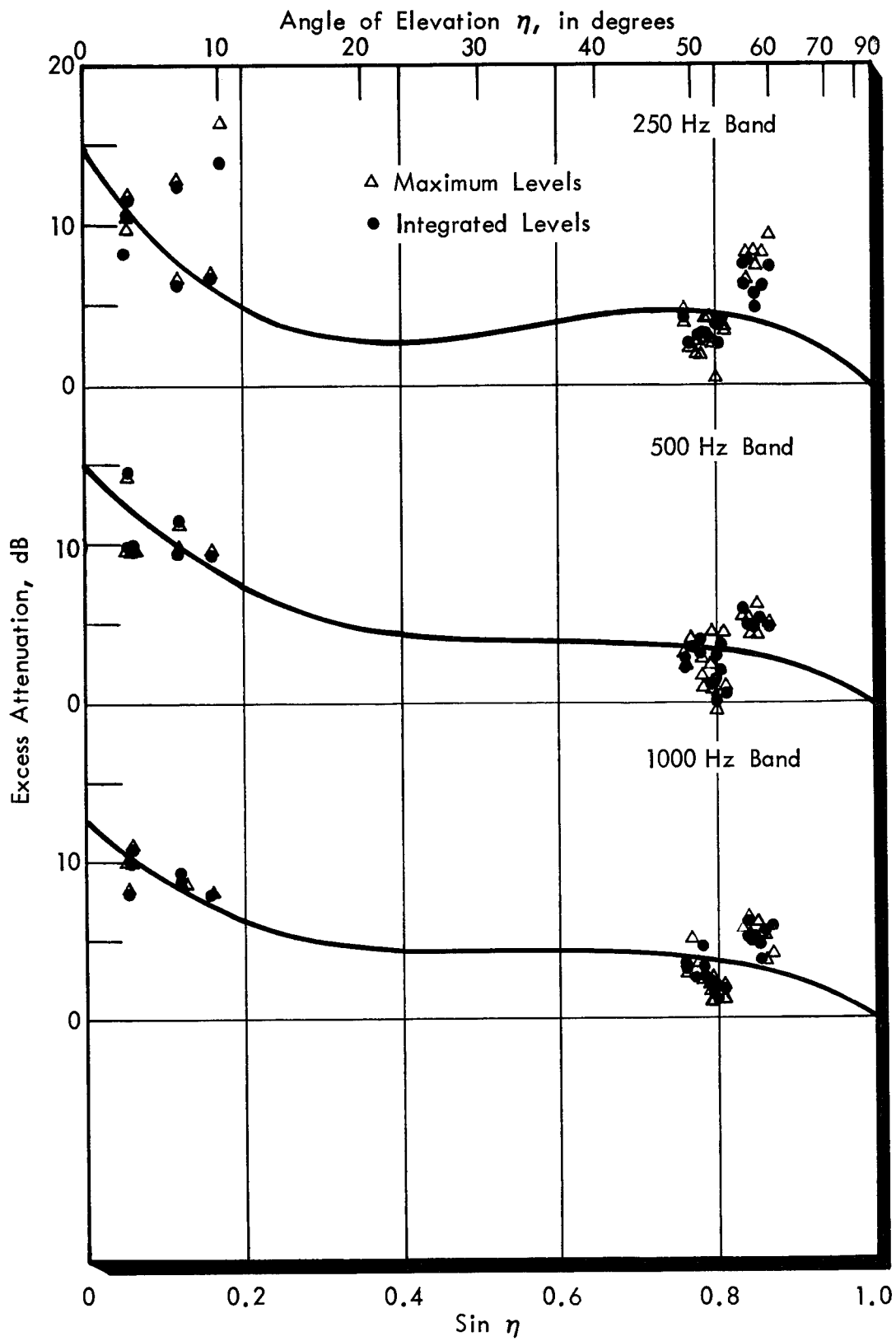


FIGURE 7. EXCESS ATTENUATION RELATIVE TO OVERHEAD MEASUREMENT POSITION - SABRELINER 65 MEASUREMENTS

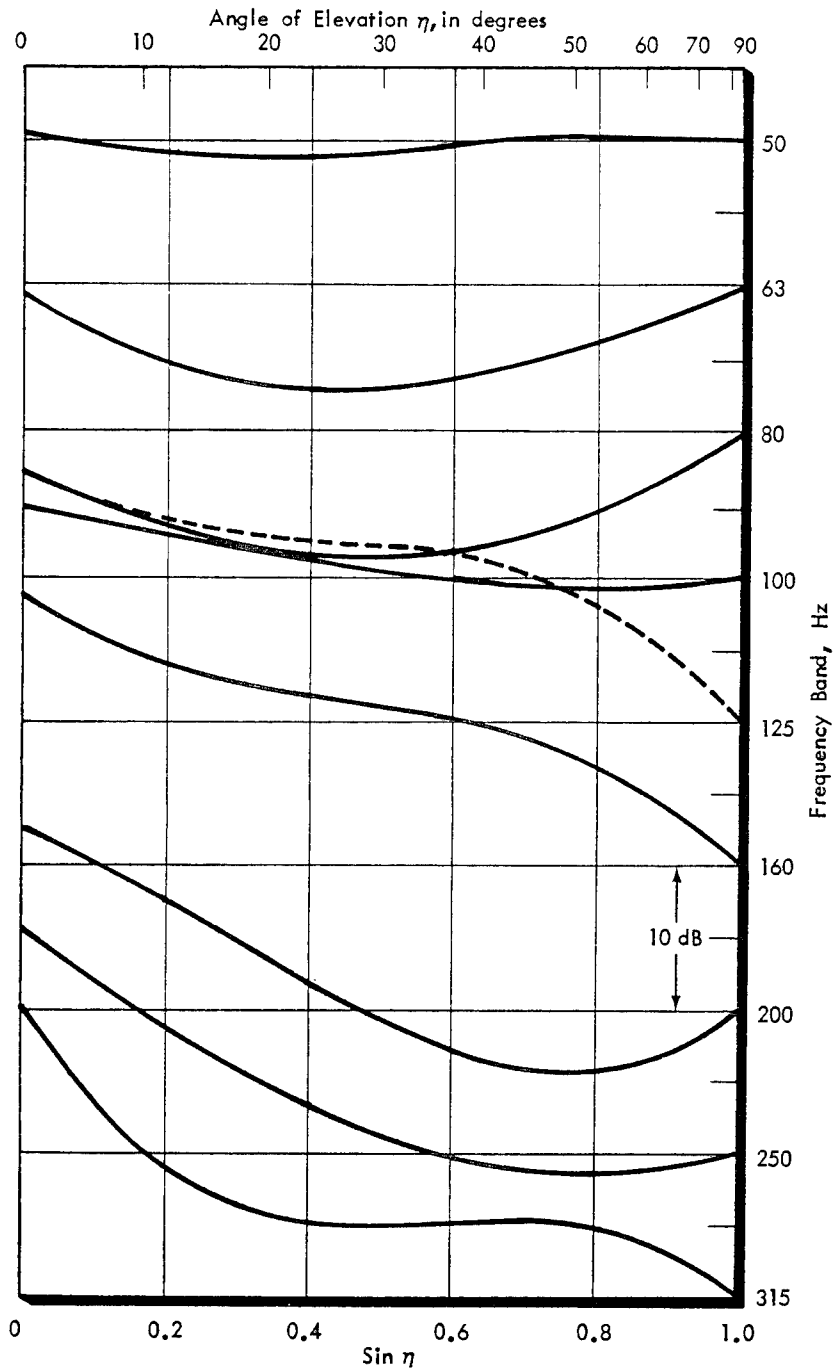


FIGURE 8-A. EXCESS ATTENUATION RELATIVE TO OVERHEAD MEASUREMENT POSITION IN ONE-THIRD OCTAVE FREQUENCY BANDS - LOCKHEED C130H

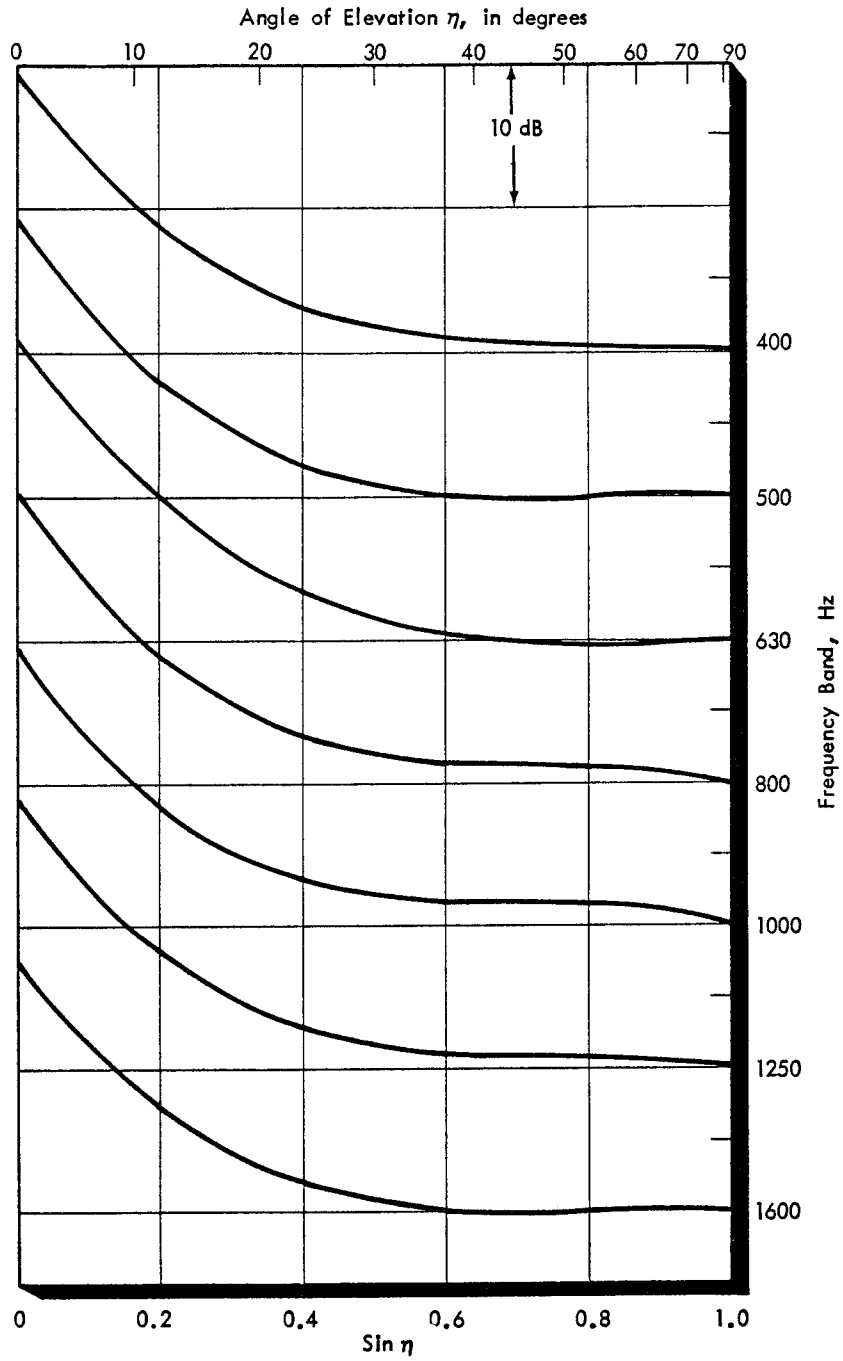


FIGURE 8-B. EXCESS ATTENUATION RELATIVE TO OVERHEAD MEASUREMENT POSITION IN ONE-THIRD OCTAVE FREQUENCY BANDS - LOCKHEED C130H

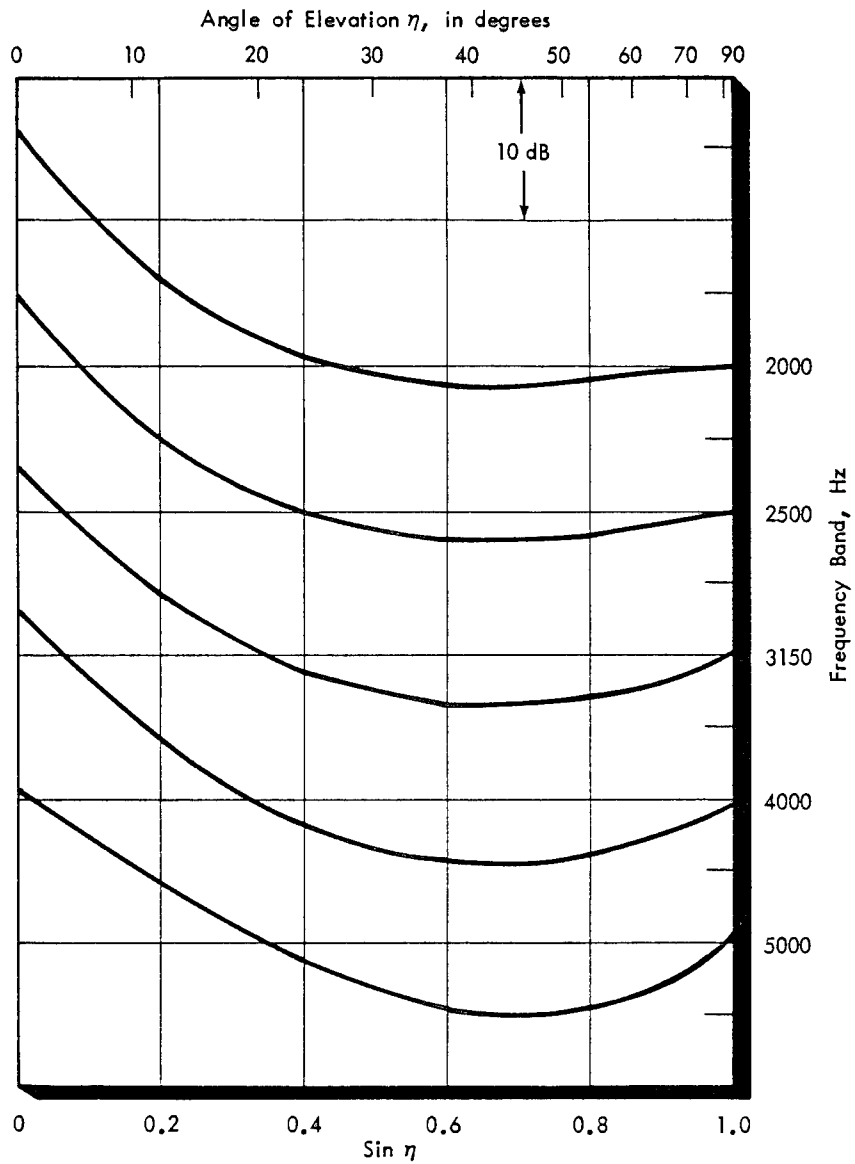


FIGURE 8-C. EXCESS ATTENUATION RELATIVE TO OVERHEAD MEASUREMENT POSITION IN ONE-THIRD OCTAVE FREQUENCY BANDS - LOCKHEED C130H

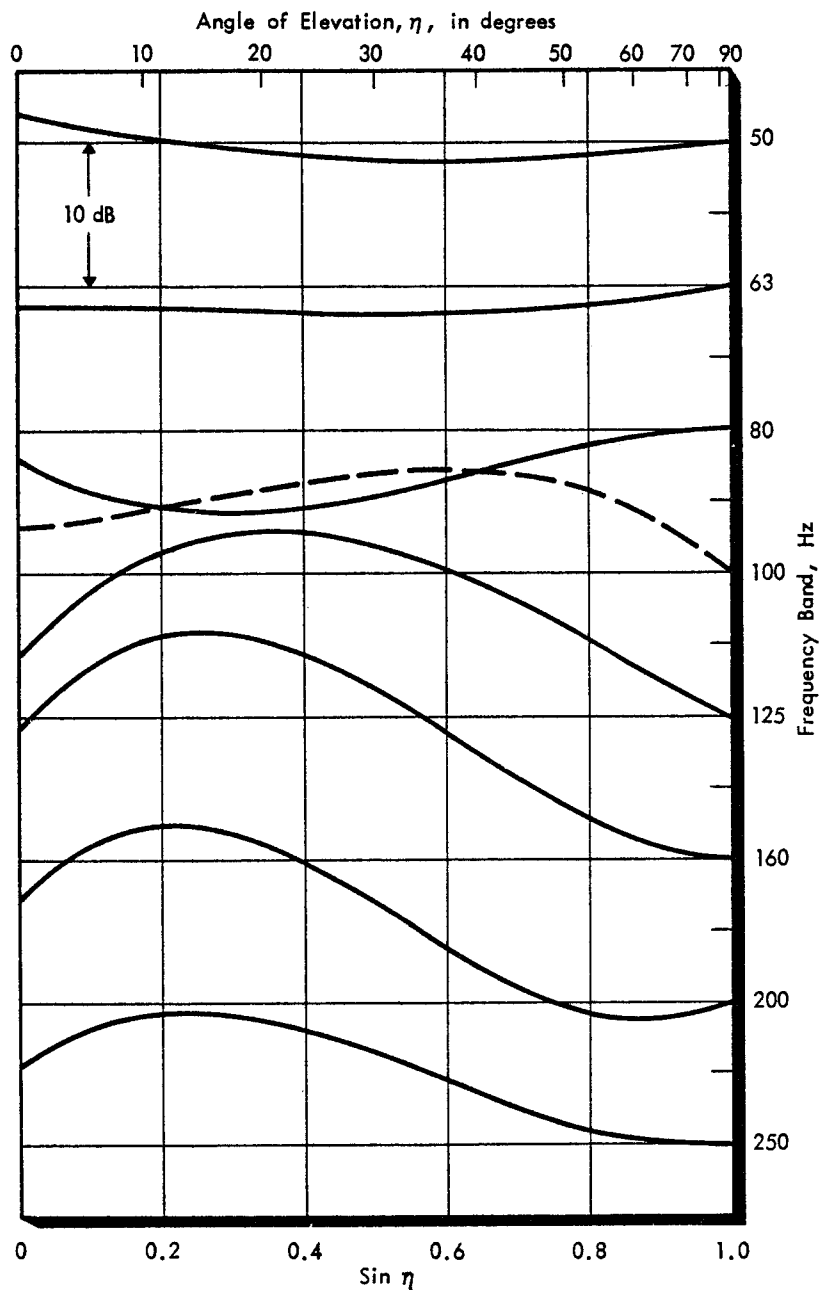


FIGURE 9-A. EXCESS ATTENUATION RELATIVE TO OVERHEAD MEASUREMENT POSITION IN ONE-THIRD OCTAVE FREQUENCY BANDS - LEARJET 24

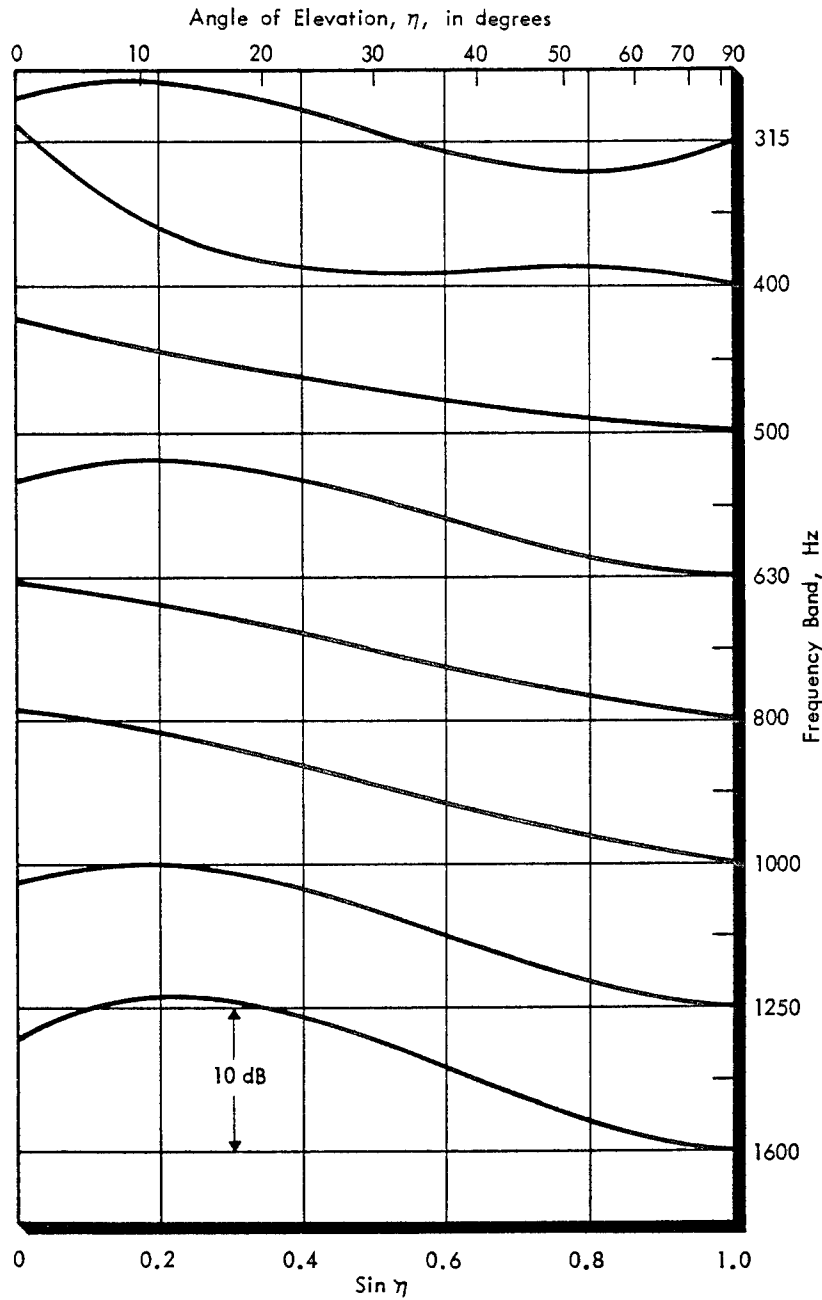


FIGURE 9-B. EXCESS ATTENUATION RELATIVE TO OVERHEAD MEASUREMENT POSITION IN ONE-THIRD OCTAVE FREQUENCY BANDS - LEARJET 24

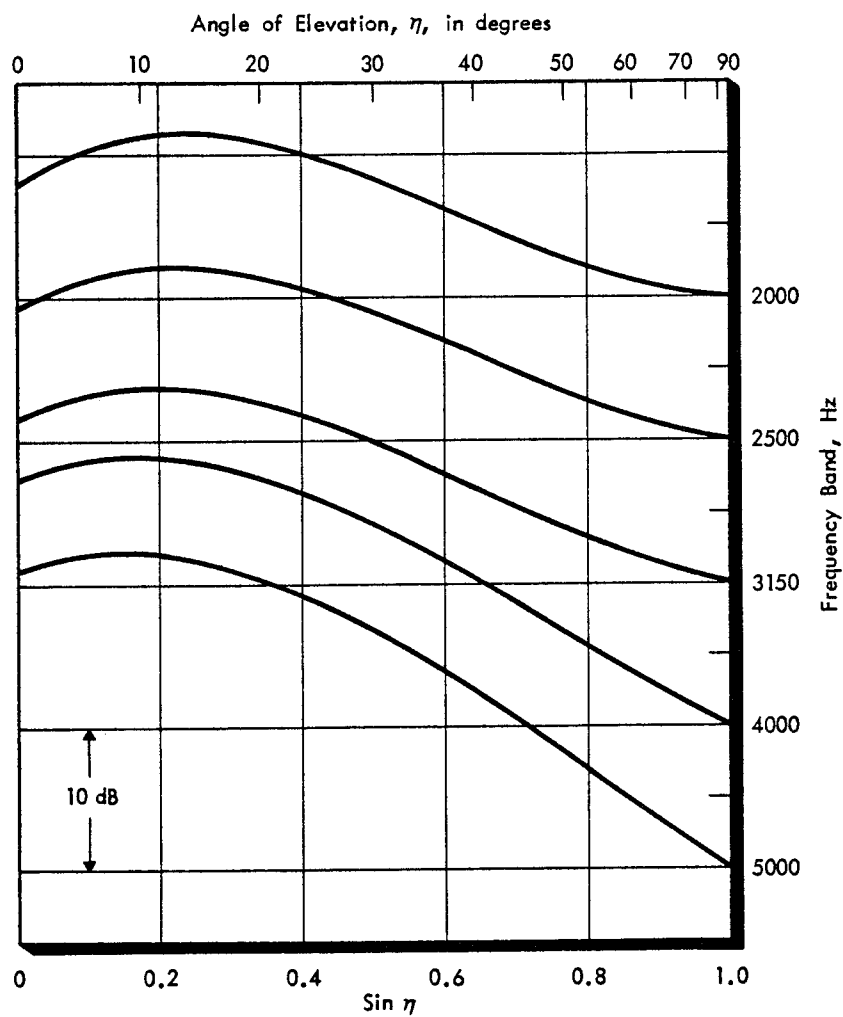


FIGURE 9-C. EXCESS ATTENUATION RELATIVE TO OVERHEAD MEASUREMENT POSITION IN ONE-THIRD OCTAVE FREQUENCY BANDS - LEARJET 24

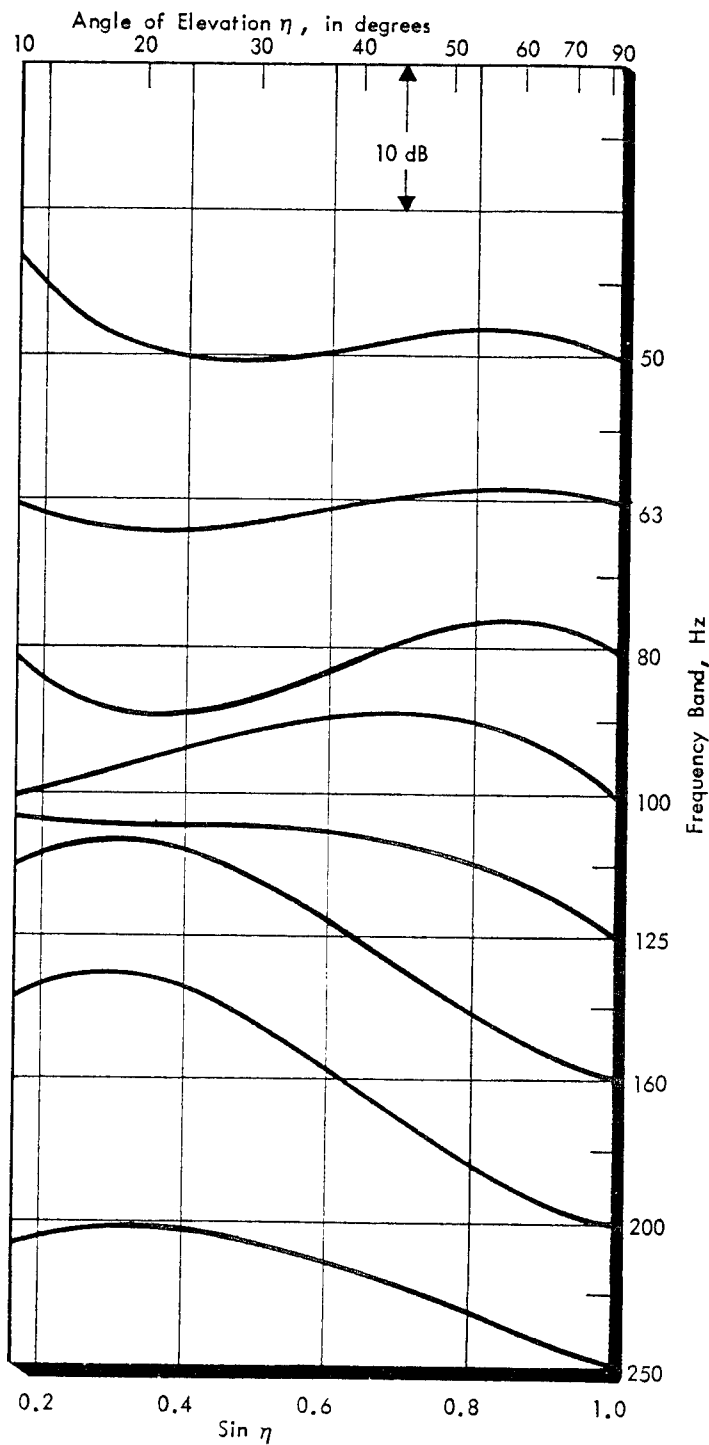


FIGURE 10-A. EXCESS ATTENUATION RELATIVE TO OVERHEAD MEASUREMENT POSITION IN ONE-THIRD OCTAVE FREQUENCY BANDS - LEARJET 24 WITH DAISY NOZZLES

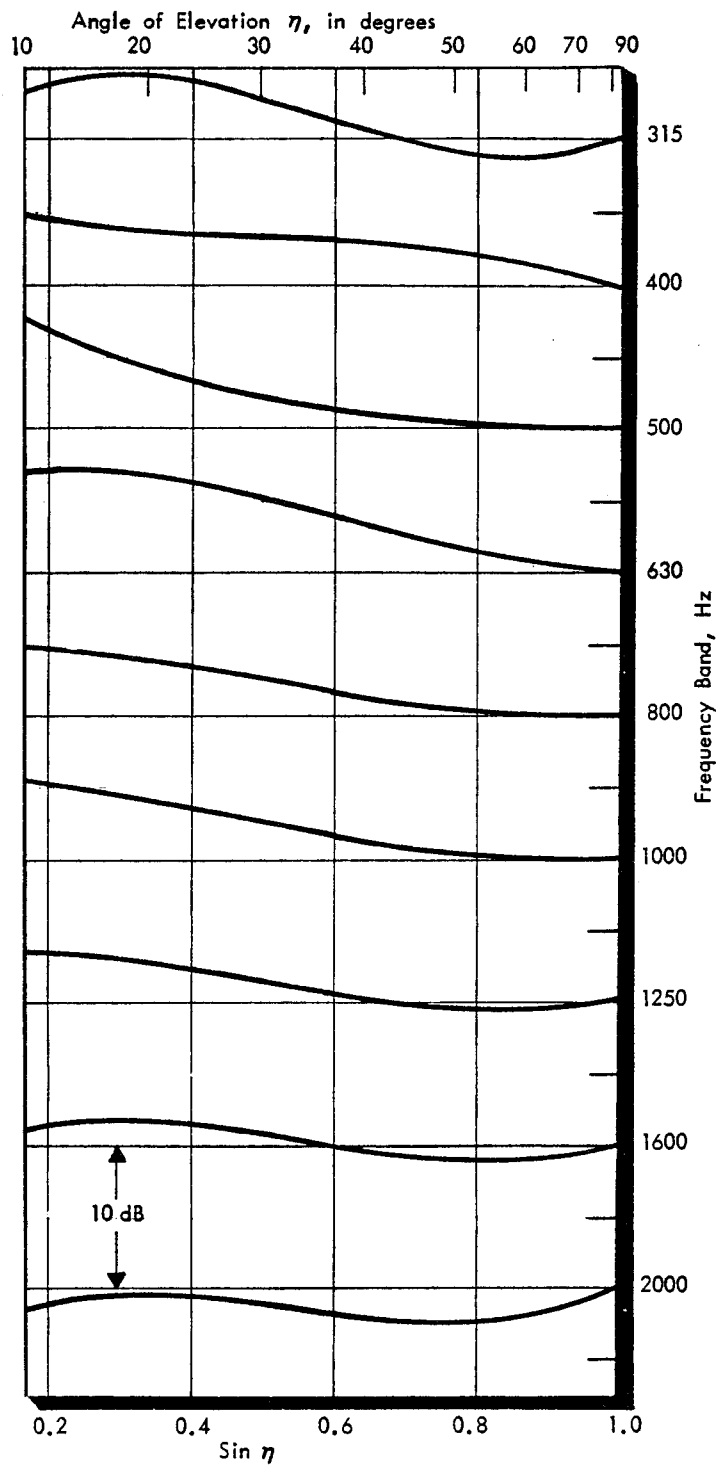


FIGURE 10-B. EXCESS ATTENUATION RELATIVE TO OVERHEAD MEASUREMENT POSITION IN ONE-THIRD OCTAVE FREQUENCY BANDS - LEARJET 24 WITH DAISY NOZZLES

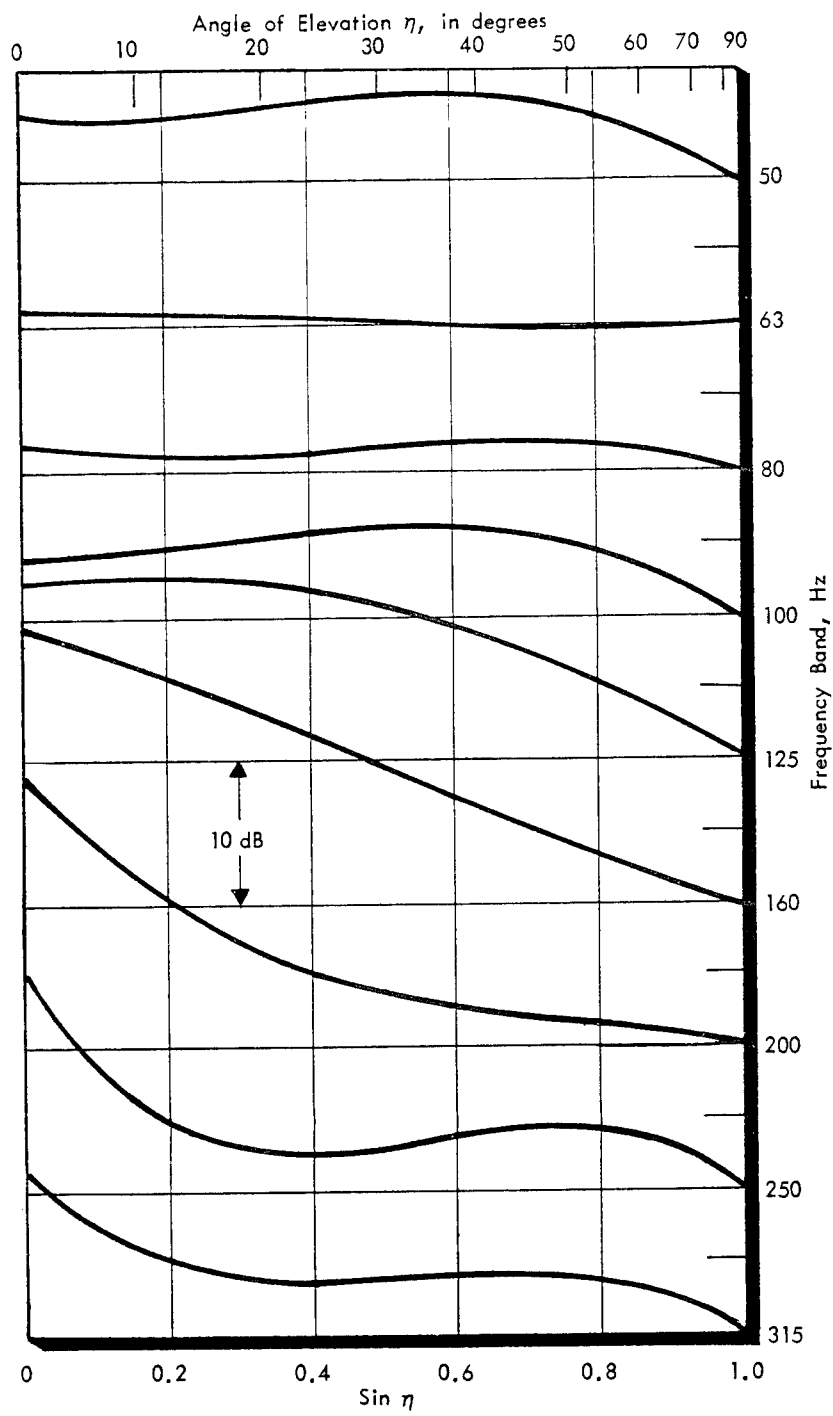


FIGURE 11-A. EXCESS ATTENUATION RELATIVE TO OVERHEAD MEASUREMENT POSITION IN ONE-THIRD OCTAVE FREQUENCY BANDS - SABRELINER 65

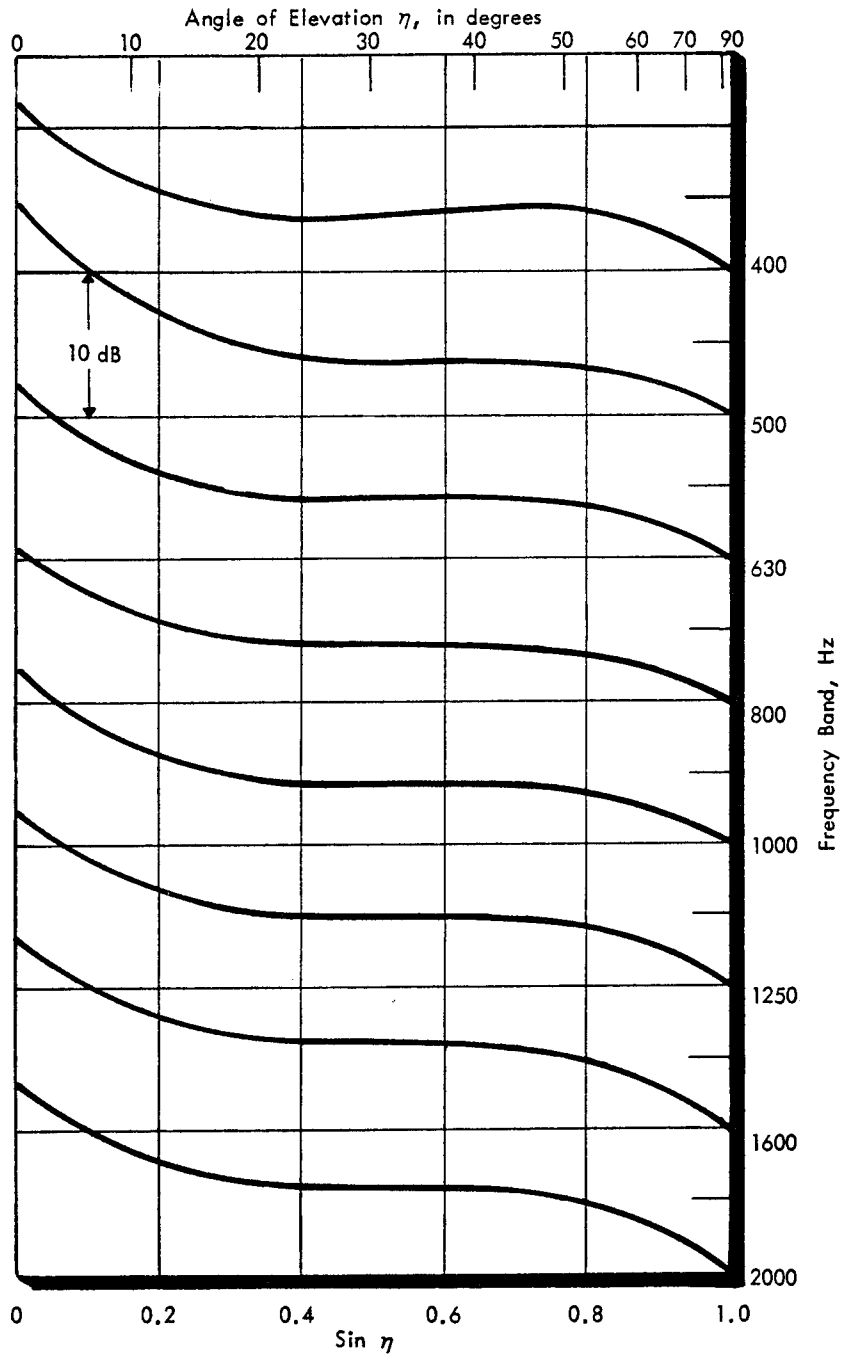


FIGURE 11-B. EXCESS ATTENUATION RELATIVE TO OVERHEAD MEASUREMENT POSITION IN ONE-THIRD OCTAVE FREQUENCY BANDS - SABRELINER 65

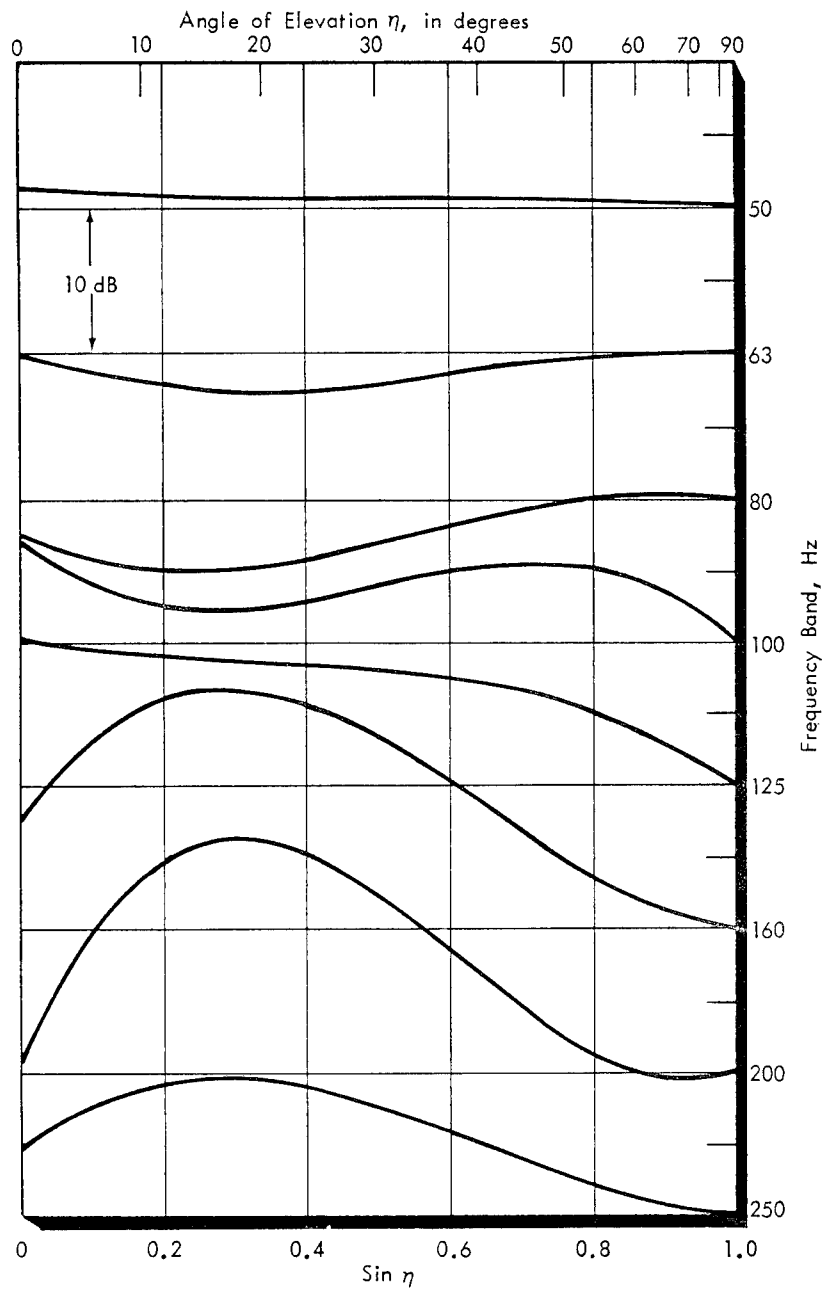


FIGURE 12A. EXCESS ATTENUATION RELATIVE TO OVERHEAD MEASUREMENT POSITION IN ONE-THIRD OCTAVE FREQUENCY BANDS - COMBINED LEARJET 24 DATA (STANDARD AND DAISY NOZZLES)

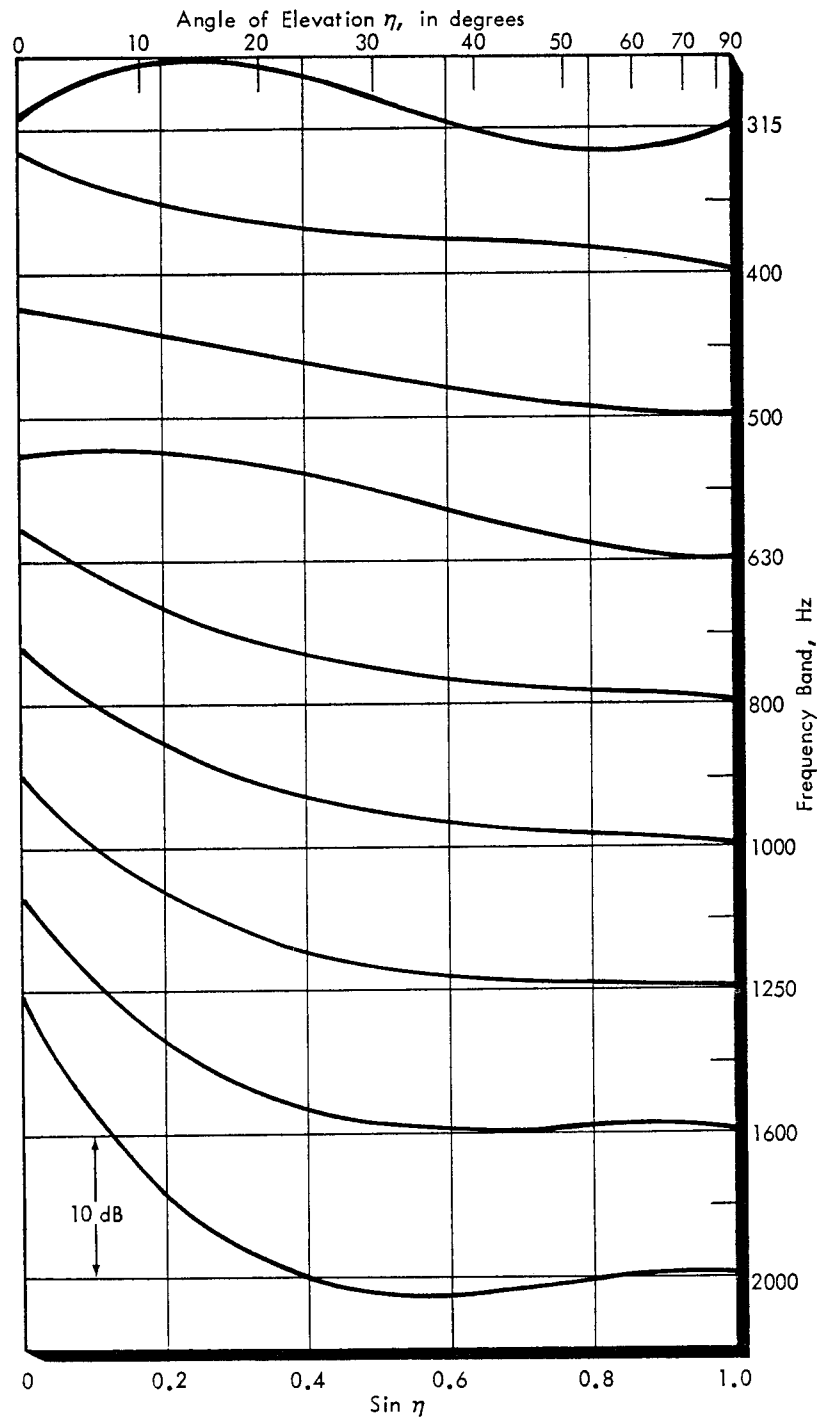


FIGURE 12B. EXCESS ATTENUATION RELATIVE TO OVERHEAD MEASUREMENT POSITION IN ONE-THIRD OCTAVE FREQUENCY BANDS - COMBINED LEARJET 24 DATA (STANDARD AND DAISY NOZZLES)

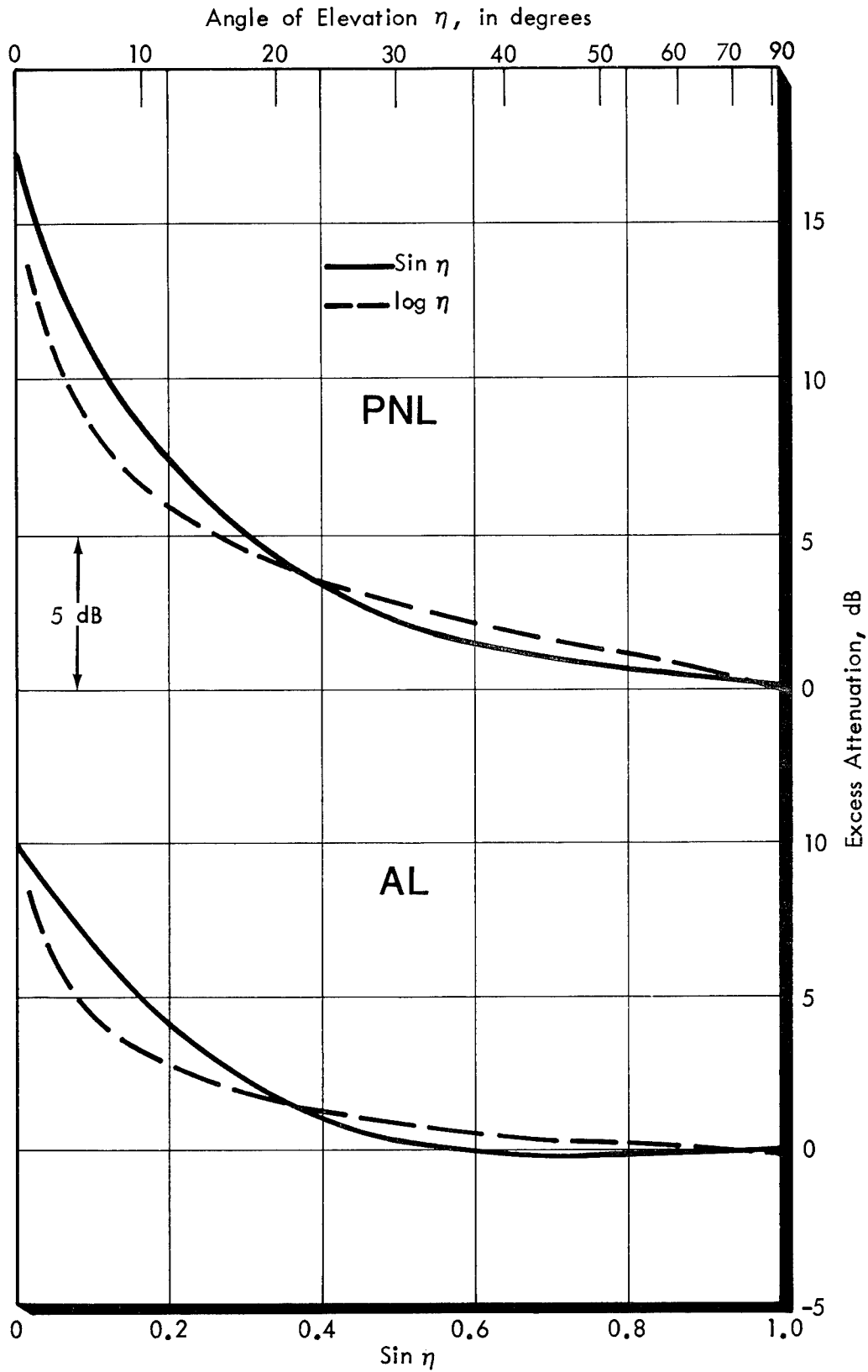


FIGURE 13. EXCESS ATTENUATION IN TERMS OF A-LEVELS AND PERCEIVED NOISE LEVELS - LOCKHEED C130H

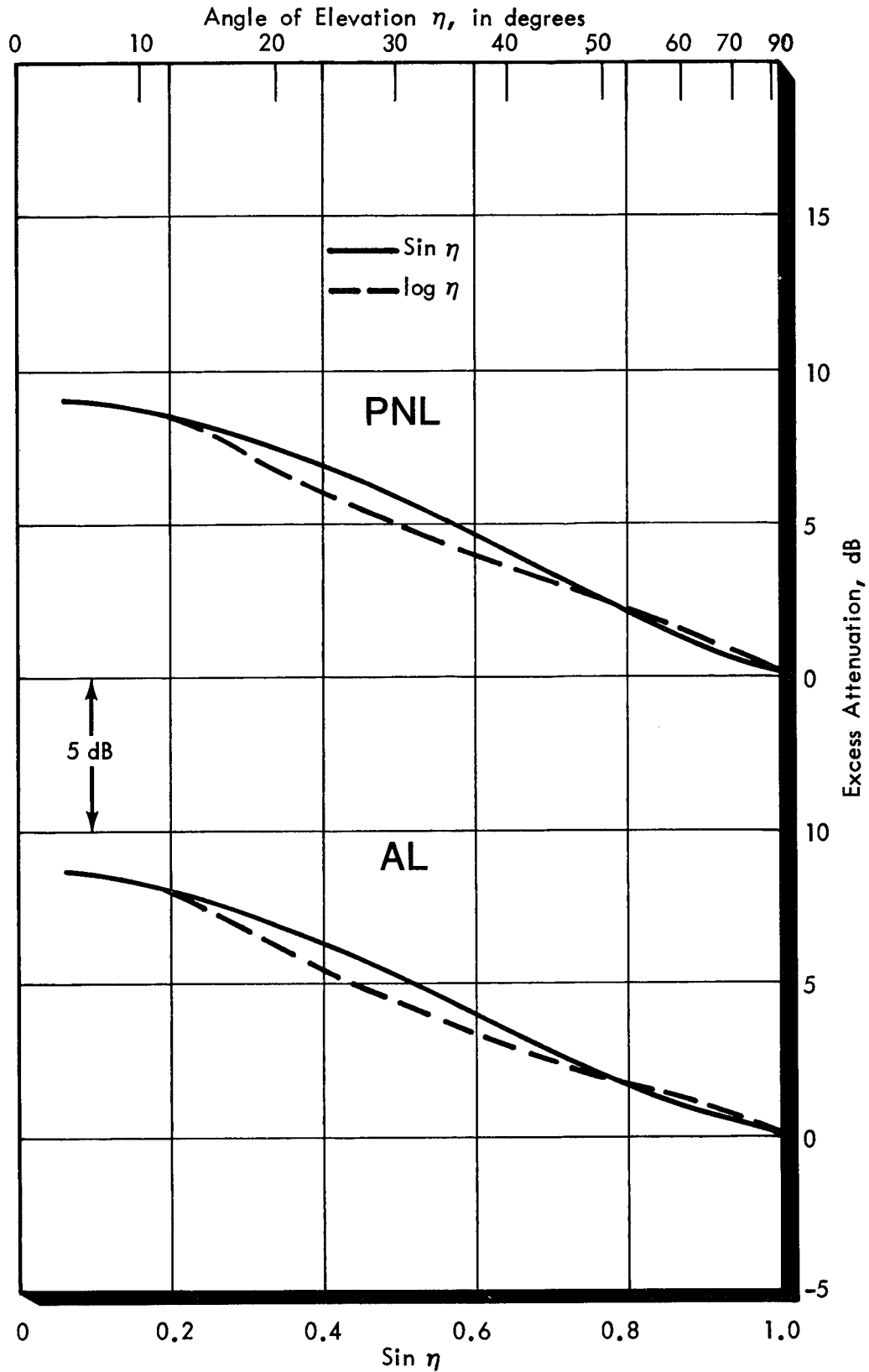


FIGURE 14. EXCESS ATTENUATION IN TERMS OF A-LEVELS AND PERCEIVED NOISE LEVELS - LEARJET 24

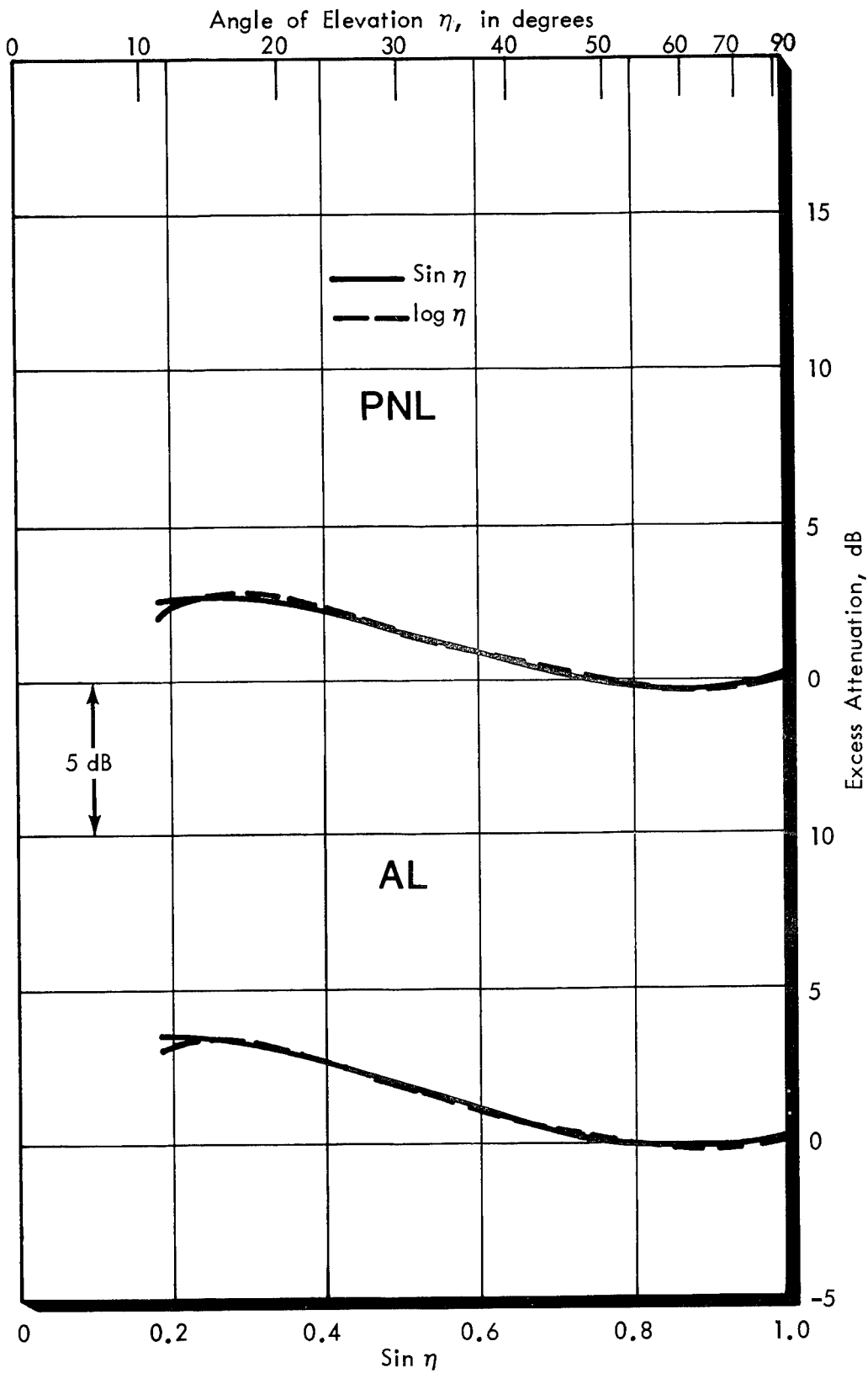


FIGURE 15. EXCESS ATTENUATION IN TERMS OF A-LEVELS AND PERCEIVED NOISE LEVELS - LEARJET 24 WITH DAISY NOZZLES

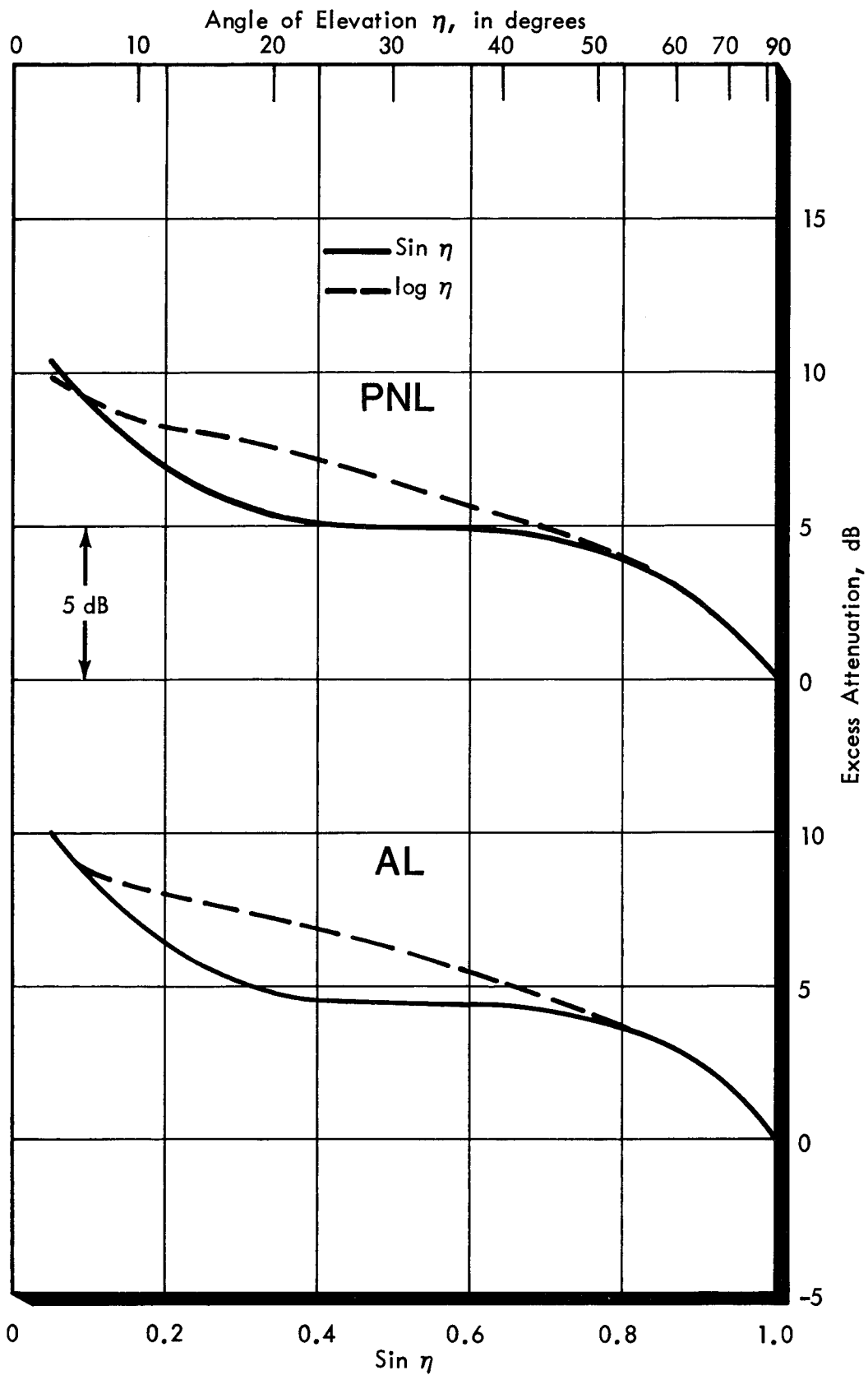


FIGURE 16. EXCESS ATTENUATION IN TERMS OF A-LEVELS AND PERCEIVED NOISE LEVELS - SABRELINER 65

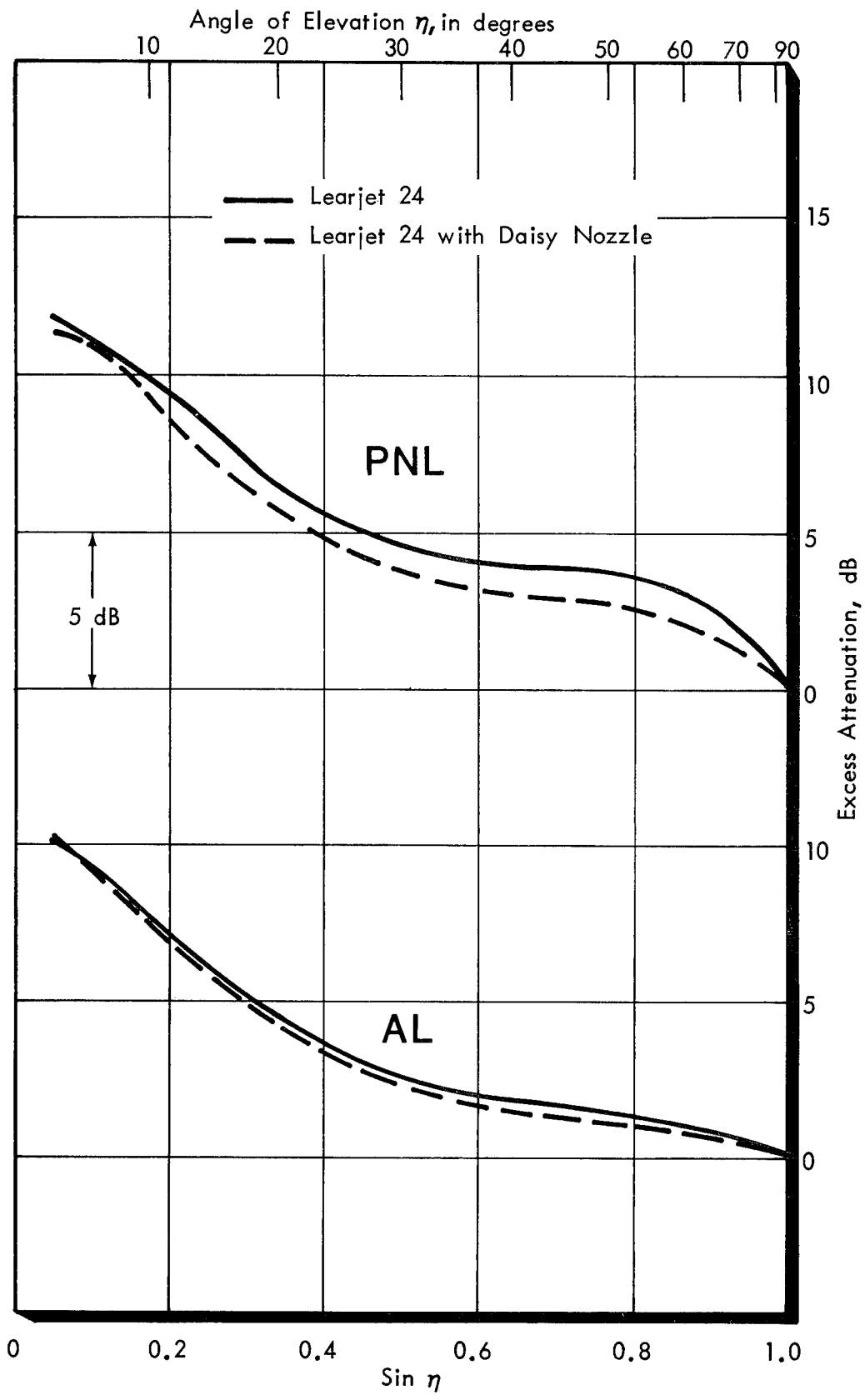


FIGURE 17. EXCESS ATTENUATION IN TERMS OF A-LEVELS AND PERCEIVED NOISE LEVELS - COMBINED LEAR 24 DATA (STANDARD AND DAISY NOZZLES)

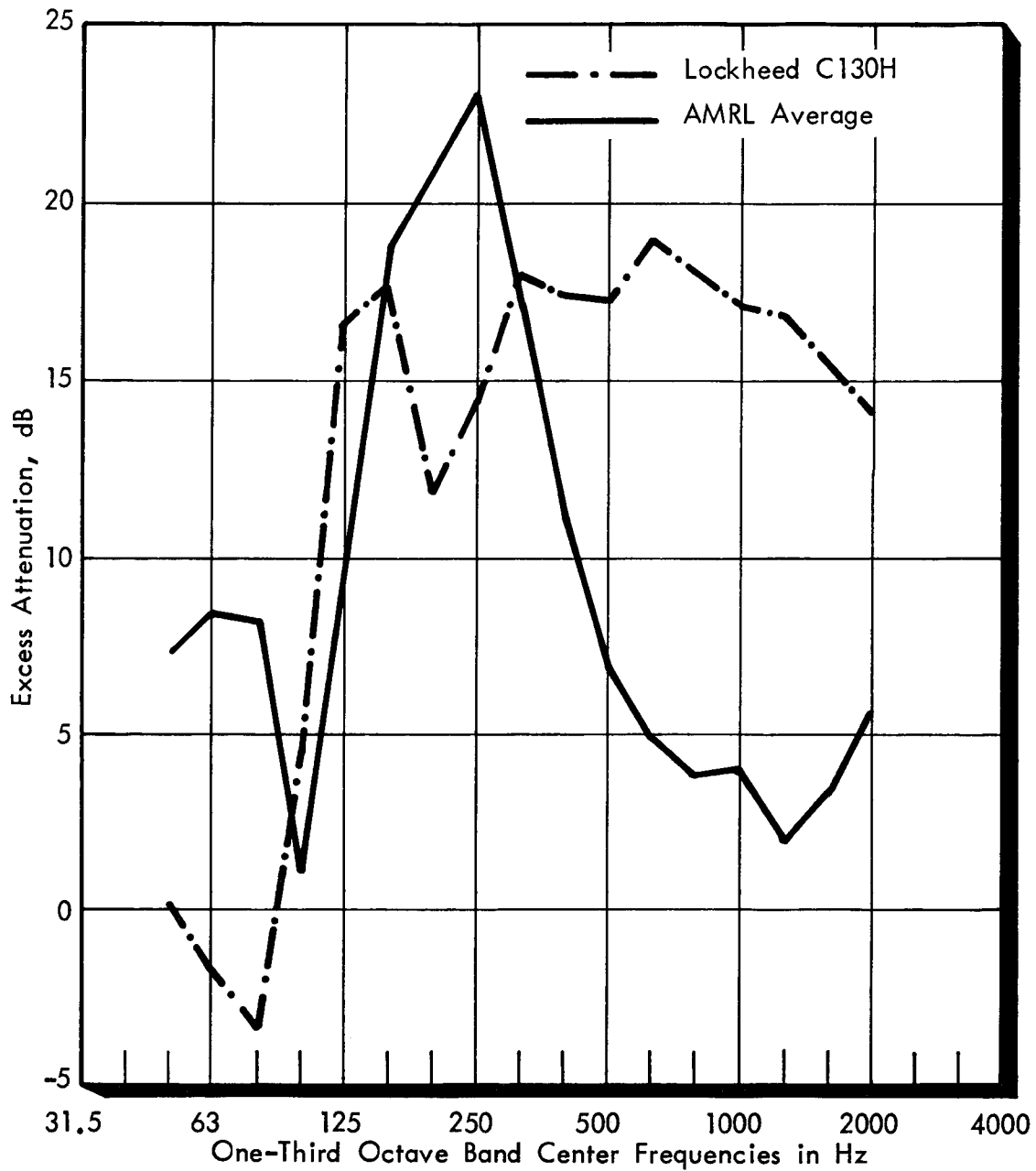


FIGURE 18. COMPARISON OF EXCESS ATTENUATION FOR TWO DEGREE ELEVATION ANGLE

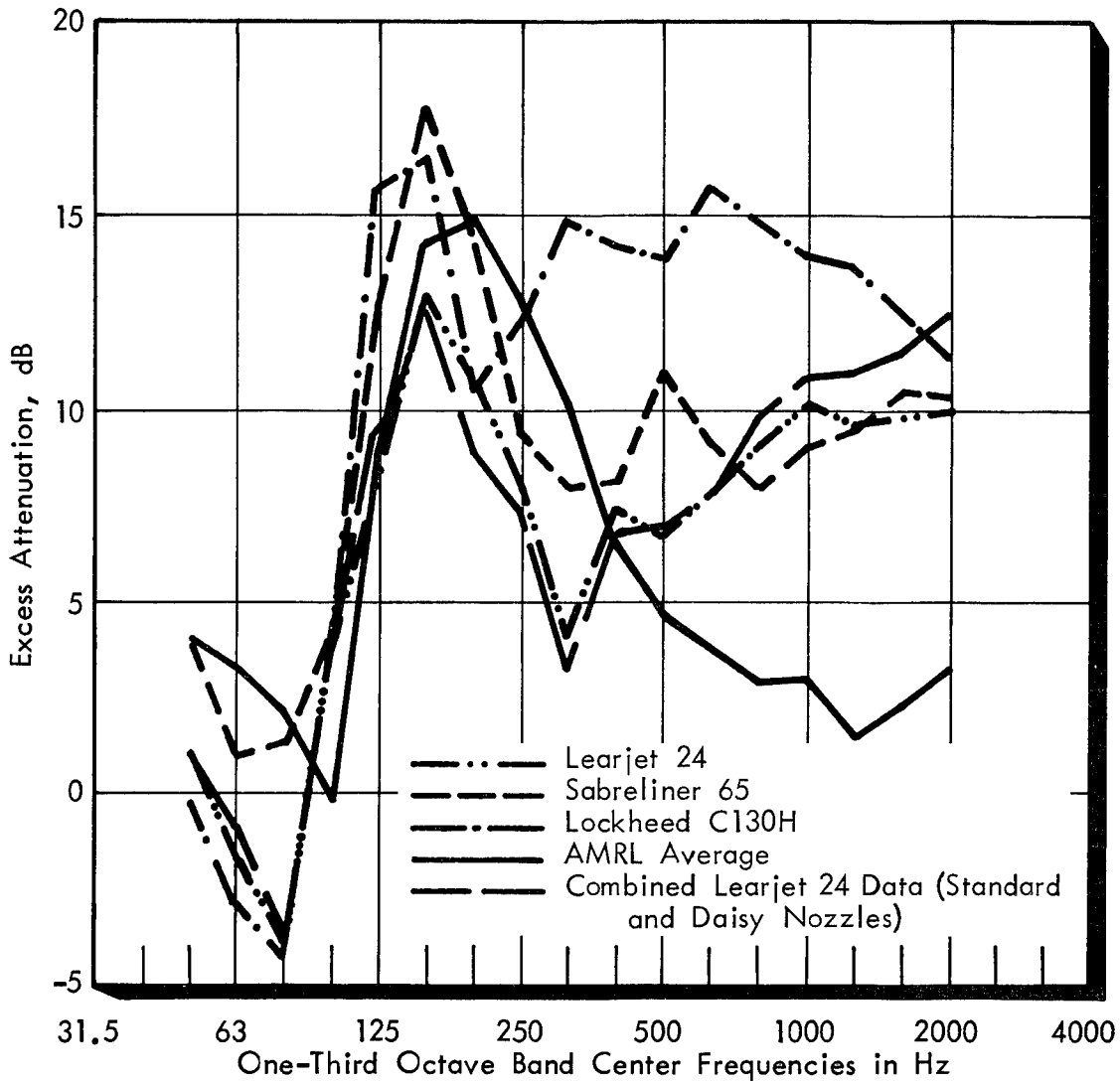


FIGURE 19. COMPARISON OF EXCESS ATTENUATION FOR FIVE DEGREE ELEVATION ANGLE

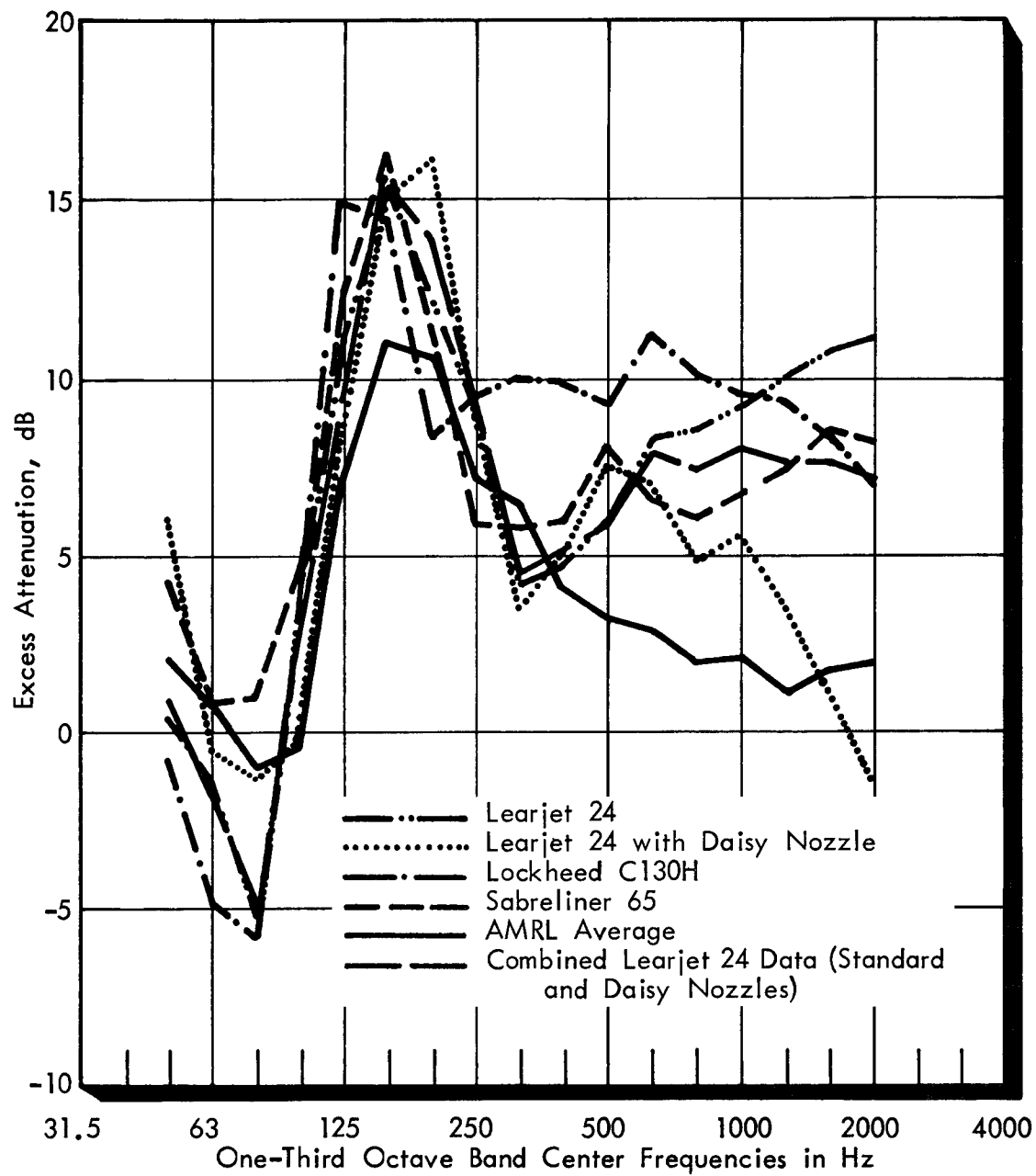


FIGURE 20. COMPARISON OF EXCESS ATTENUATION FOR TEN DEGREE ELEVATION ANGLE

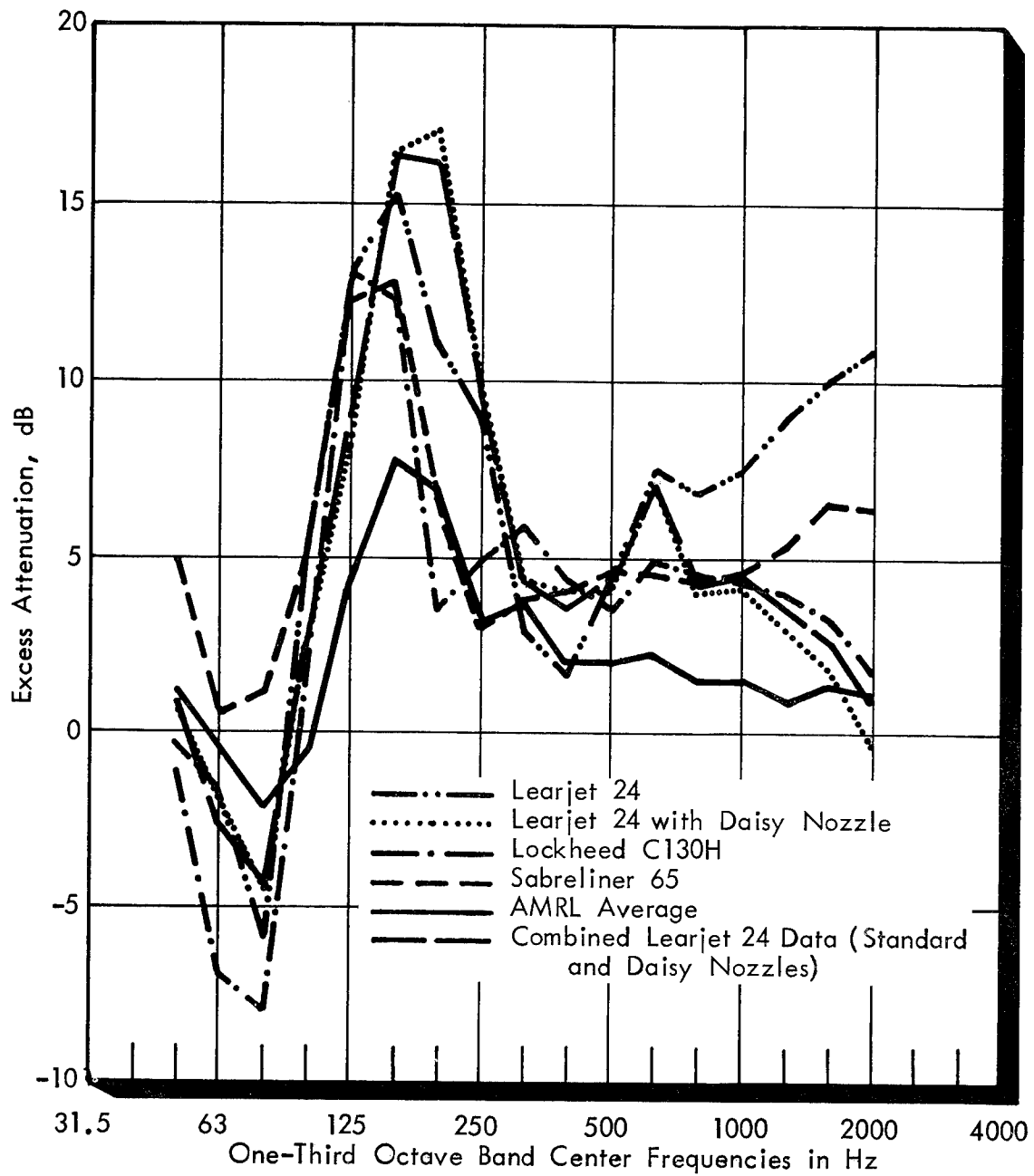


FIGURE 21. COMPARISON OF EXCESS ATTENUATION FOR TWENTY DEGREE ELEVATION ANGLE

recently (and informally) by the Air Force Aerospace Medical Research Laboratory, based on measurements of a number of military aircraft.*

The final set of figures, Figures 22 through 25, show the average normalized noise spectra at the overhead position for each aircraft. Two spectra are shown, one based on maximum levels and the other based on the integrated levels, after adjustments. Also shown in these figures is the standard deviation for the average spectra. With minor exceptions evident particularly at frequencies below 150 Hz, the normalized spectrum based on maximum levels agrees very closely with that based upon integrated levels. The variability in measurements is approximately the same for both the composite (maximum) spectra and the integrated spectra, with the standard deviations typically averaging less than 2 dB over most of the frequency range.

DISCUSSION

Figures 4 through 7 illustrate typical variability in data and also show the clustering of data with angle encountered in the certification measurements. The distribution of data versus elevation angle differs markedly among the four sets of certification tests. As a result, some of the certification tests were more useful than others, since data was available over a wide range of angles.

Figure 4, for the C-130, shows relatively good distribution of data with angle with clustering of data between 0 to 5°, 15 to 20°, and 30 to 40°. This distribution allows the excess attenuation to be determined over a relatively wide range of elevation angles.

Figure 5, for the Lear 24, shows clustering in the vicinity of 5 to 10° and between 50 to 55° with no data between. For the Lear 24 with daisy nozzles, the data is also clustered in two groups, between 10 to 25°, and between 45 to 60°. There are gaps between the groups, with no data below 10°. The Sabreliner 65 data, Figure 7, shows clustering of the data between 3 to 10° and between 50 to 60°.

Figures 4 through 7 also show the similarity in excess attenuation data obtained from comparisons of maximum levels and comparisons of integrated levels. Because there was no evident systematic difference between maximum and integrated level data, the regression curves were calculated using both sets of data.

The excess attenuation curves for one-third octave bands between 50 to 2000 Hz, (Figures 8 through 12) generally show considerable variation in shape at low frequencies (between 50 to 200 Hz) with

* The AMRL curve is the average of measurements of several level flyovers of different aircraft (A-10, C-135A, C-141, E-3A, F-5E, F-15, F-18). Data for the individual aircraft show variations of the order of +3 to +5 dB about the average curve.

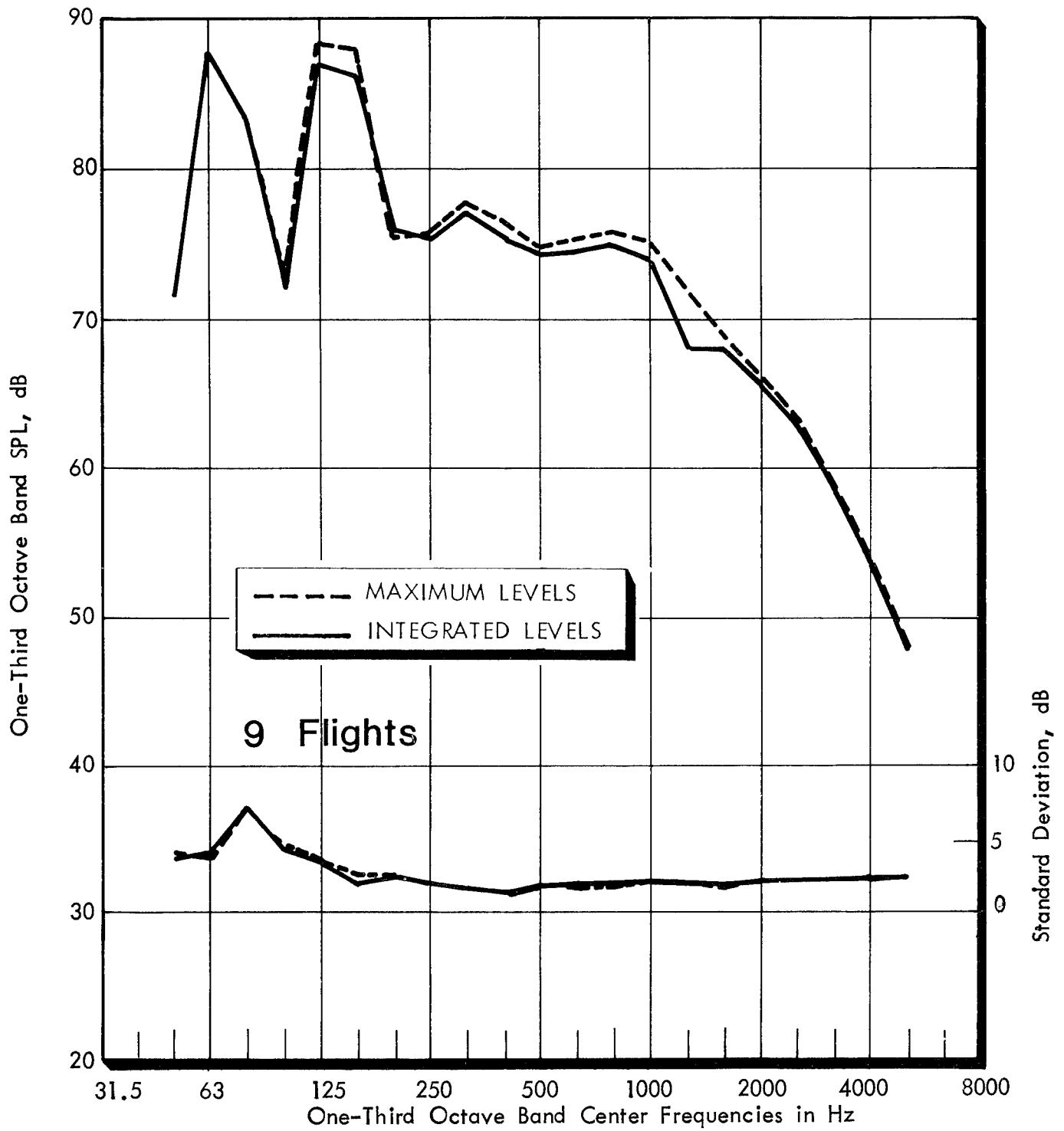


FIGURE 22. AVERAGE NORMALIZED NOISE SPECTRA AT OVERHEAD POSITION (90° ELEVATION ANGLE, 2000 FEET DISTANCE) - LOCKHEED C130H

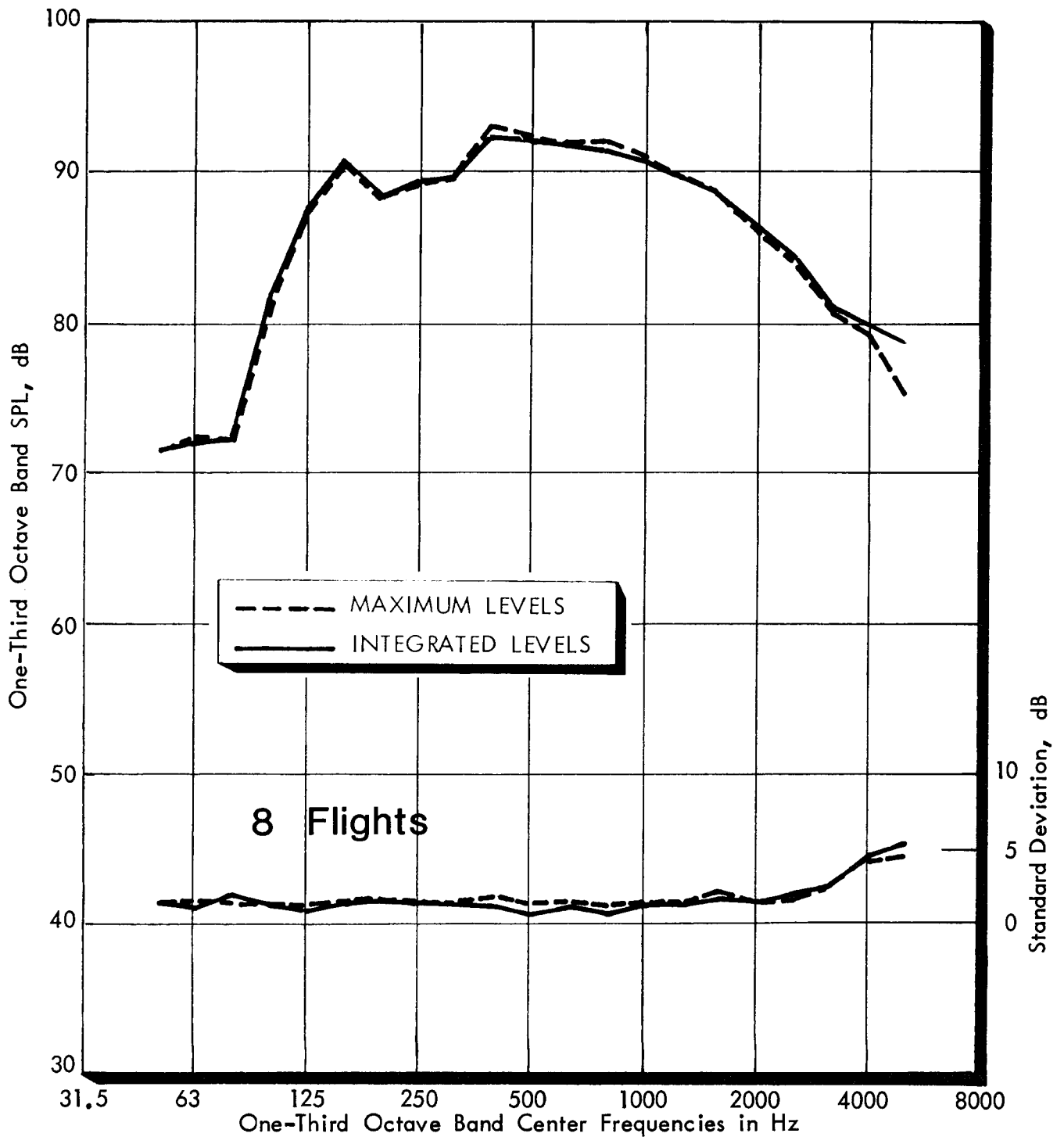


FIGURE 23. AVERAGE NORMALIZED NOISE SPECTRA AT OVERHEAD POSITION (90° ELEVATION ANGLE, 2000 FEET DISTANCE) - LEARJET 24

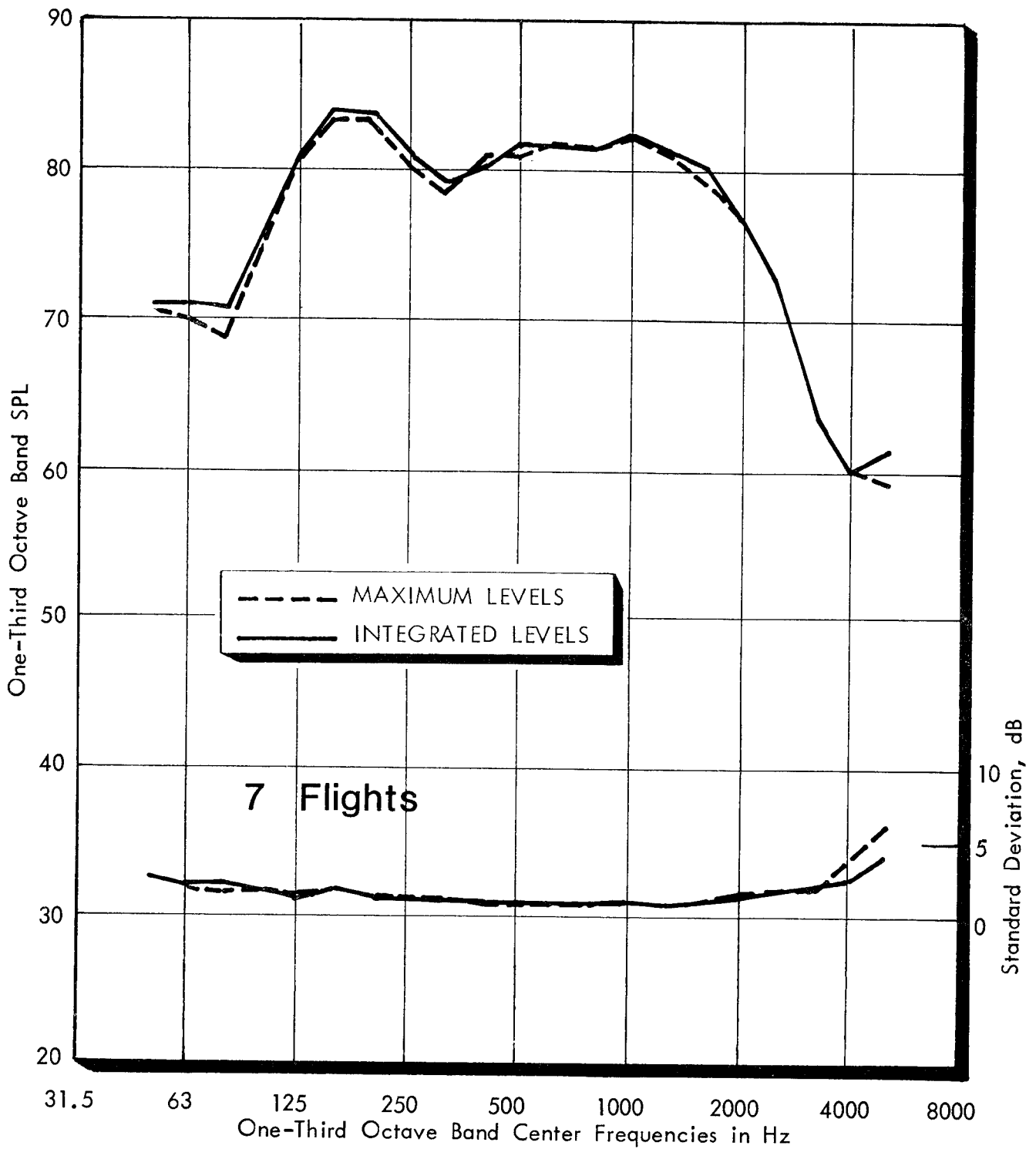


FIGURE 24. AVERAGE NORMALIZED NOISE SPECTRA AT OVERHEAD POSITION (90° ELEVATION ANGLE, 2000 FEET DISTANCE) - LEARJET 24 WITH DAISY NOZZLES

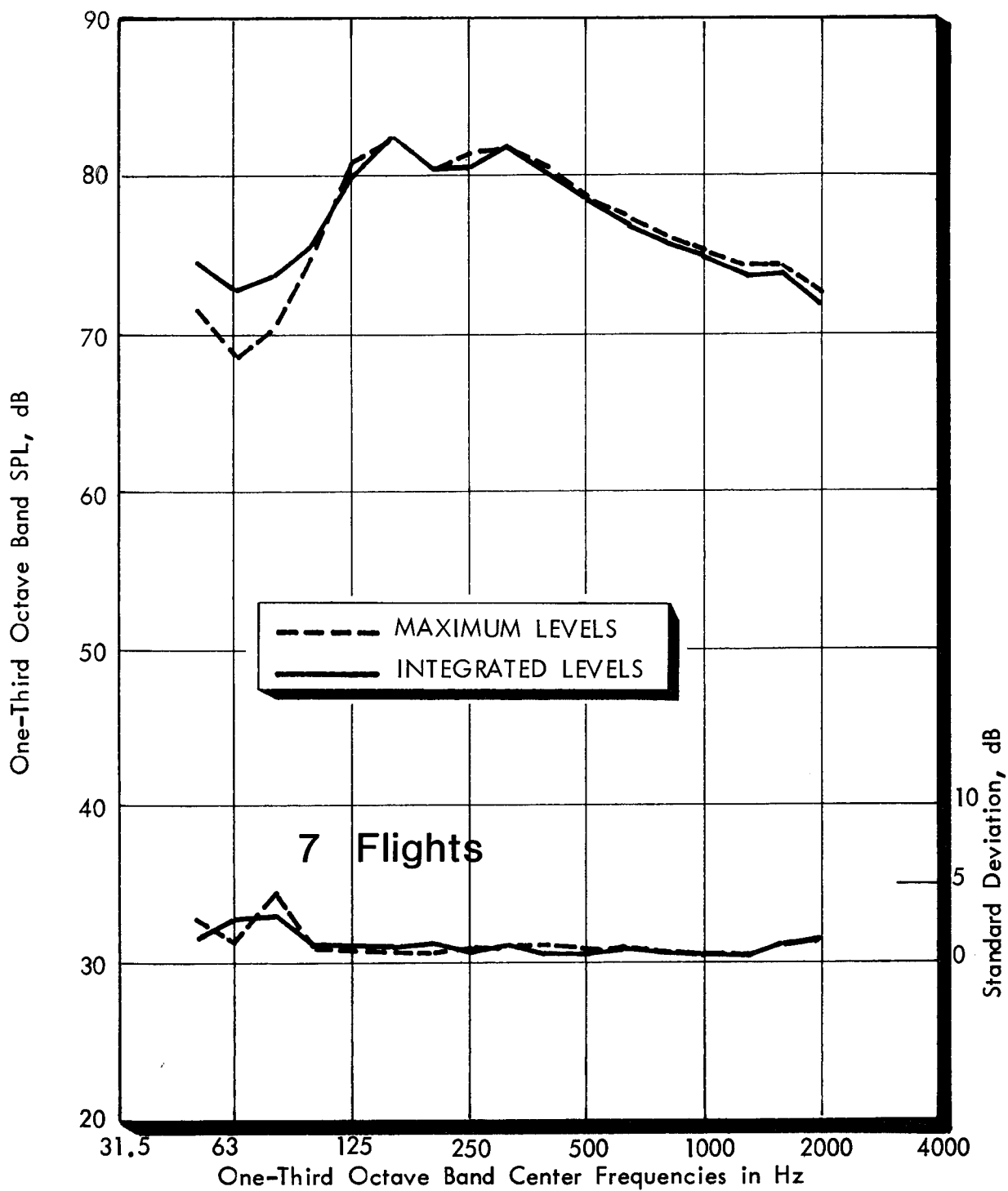


FIGURE 25. AVERAGE NORMALIZED NOISE SPECTRA AT OVERHEAD POSITION (90° ELEVATION ANGLE, 2000 FEET DISTANCE) - SABRELINER 65

relative consistency in shape from one-third octave band to another in higher frequencies. For the sets of data in which measurements were clustered in two small ranges of elevation angles (Lear 24, Lear 24 with daisy nozzles, and Sabre 65), the regression curves based upon a three degree polynomial may show curve details not substantiated by the data (i.e., lower order regression curves would have provided equally valid fits to the data). For the sets of data with a better distribution of measured excess attenuation with angle (the C-130 and the combined Learjet 24 data), the calculated regression curves have better validity.

Figures 13 through 17, showing the excess attenuation in terms of PNL and AL, summarize the results of the analysis in terms of widely used aircraft noise measures. In Figures 13 through 16, the differences in curves based on $\sin \eta$ and $\log \eta$ regression assumptions are not large, except for the Sabre 65 (Figure 16).

It should be remembered that the excess attenuation curves are based upon the comparison of both maximum levels and integrated levels. Hence, although the curves of Figure 13 through 17 are labeled A-level and PNL, the excess attenuations should apply to SEL data and also to EPNL data (except for the influence of possible tone corrections for the latter). Note that no special assumptions other than inverse square spreading were made in adjusting data to reference conditions (i.e., no duration assumptions* were imposed in adjusting the integrated data).

Although the shapes of the A-level and PNL excess attenuation curves for each aircraft are generally similar, the magnitudes of the excess attenuation at any given angle generally differs, with the excess attenuation expressed in terms of PNL usually being larger than the AL values. This difference is particularly evident for the C-130 (Figure 13) and for the curves based on the combined Learjet 24 data (Figure 17).

Comparison of the PNL and AL curves derived from the individual sets of Lear 24 test data (Figures 14 and 15) show sizeable differences in the magnitude of the excess attenuation and in details of the curve shape. The Learjet 24 (standard nozzles) shows much higher excess attenuation in the vicinity of 10 to 20 degrees, as a consequence of the measurements clustered in the vicinity of 5 to 10 degrees. Curves for the Learjet 24 with daisy nozzles show lower excess attenuation at small elevation angles, reflecting the absence of data at lower elevation angles.

* Because the ranges in slant distance were small, magnifying the effect of small differences in measured levels in calculating duration adjustments, the calculated variation of the duration adjustment with distance ("slope" of the duration adjustment) showed quite high variability among frequency bands. Thus, the "slope" values showed much greater variability than observed from analysis of measurements over larger distance ranges.

The PNL and AL curves based upon the combined Lear 24 test data (Figure 17) are quite different in shape from the curves based on the individual test sets. Combining the test data results in improved definition of the excess attenuation over the angular range from about 5° to 25°. The curves of Figure 17 show small differences between aircraft which result solely from the differences in the shape of the overhead noise spectra for the two aircraft (compare Figures 23 and 24).

The Sabreliner 65 shows relatively high excess attenuation (order of 3 to 5 dB) at high elevation angles, (ranging up to 60°). This trend is clearly evident in the measured data shown in Figure 7. The reasons for the relatively high excess attenuation at high elevation angles for the Sabreliner 65, in contrast to other aircraft, is not known. However review of other certification tests for this aircraft indicate a similar phenomenon (i.e., the sideline levels at relatively large elevation angles are lower than anticipated with reference to the overhead levels).

Figures 18 through 21 show the computed excess attenuation (as read from the regression curves) as a function of frequency and provide insight as to the reasons for the differences in the PNL and A-level curves as a function of angle. Figure 18 compares the excess attenuation for the C-130 with the average curve obtained by AMRL from analysis of recent military aircraft data. Note that the characteristic shape of the curves is quite different in that the C-130 measurements show higher excess attenuation at higher frequencies (about 315 Hz) than does the Air Force data. Both curves show relatively large excess attenuations in the range from approximately 125 Hz to 315 Hz.

Figure 19, for a 5° elevation angle, shows four sets of curves in comparison with the AMRL average curve. All of the curves derived from certification data show higher excess attenuations than the AMRL curve for frequencies above approximately 400 Hz. Note, however, that all data (certification and AMRL) show a characteristic peak in excess attenuation in the vicinity of 160 to 200 Hz with a sharp dropoff in excess attenuation at lower frequencies.

Figures 20 and 21, showing excess attenuation for 10° and 20° elevation angles, also show similar trends. These curves show little excess attenuation at 100 Hz or lower, a distinct maximum in excess attenuation in the frequency range from 125 Hz to 200 Hz, with lower attenuation at higher frequencies. Again, all of the certification data shows higher excess attenuations at frequencies above about 400 Hz.

It should be noted that the relatively consistent "peak" in excess attenuation generally noted in the range of 160 to 200 Hz is due, in large part, to ground reflections resulting from the finite microphone height (1.2m) used for both the certification and Air Force measurements.

CONCLUSIONS

This study illustrates that useful excess attenuation information can be developed from aircraft certification data. However, unless special planning steps are taken in locating the sideline positions, the measurements from sideline locations will not necessarily cover the range of low elevation angles where excess attenuation is most important and where the changes in excess attenuation with elevation angle are likely to occur most rapidly.

The spread in excess attenuation data, when analyzed in terms of one-third octave bands is quite reasonable, and the availability of the repeat flights, required for certification tests, provides a very useful data base.

The excess attenuation values determined from composite (maximum) flyover values and those derived from time integrated levels show little difference.

The measured excess attenuation generally showed trends with frequency that are consistent with the measurements observed in recent Air Force tests in the frequency range up to about 400 Hz (this includes relatively moderate excess attenuation and even negative values in the frequency range of 100 Hz or lower and a maximum in the excess attenuations, largely attributable to the finite microphone height, in the range of 160 to 200 Hz). The analysis of certification data showed larger excess attenuations than the Air Force measurements in the frequency range above 400 Hz extending up to 2000 Hz. The reasons for this difference are not known.

The perceived noise level and A-level excess attenuation versus elevation angle curves for the four aircraft studies are generally similar in shape. However the excess attenuation values for PNL were generally slightly larger than the AL values. The difference in excess attenuation values for PNL and AL was most pronounced for the C-130 aircraft.

APPENDIX

EXCESS ATTENUATION CALCULATION
STEPS AND EQUATIONS

APPENDIX

EXCESS ATTENUATION CALCULATION STEPS AND EQUATIONS

The appendix lists the calculation steps and the equations used to obtain the excess attenuation data presented in the "Presentation of Data" section of the report. The working equations may be broken into three groups:

- (a) Sideline position calculations
- (b) Takeoff position calculations
- (c) Spectrum adjustment calculations

The various geometrical distances and angles are identified in Figures 2 and 3 of the report. Throughout, as indicated in the figures, the basic reference distance is the slant distance, h . Note that this slant distance, h , does not correspond to the distance to the point of closest approach of the aircraft during the takeoff. (The distance to point of closest approach is given by the quantity $h \cdot \cos \gamma$). This reference distance was chosen because it is identified in the certification noise measurement tapes, and is particularly relevant in determining the time the aircraft was abreast of the aircraft (sideline position) or directly overhead (takeoff position).

The important quantities determined in the sideline and takeoff calculations are the elevation angle η , the slant distance h , and the distance z (sideline) or x (takeoff) which are used to calculate adjustments for air absorption. Other quantities, such as the angle of maximum radiation from the aircraft, were also determined but are not required for the excess attenuation calculations.

CALCULATION STEPS FOR SIDELINE POSITION (SEE FIGURE 2)

1. List T_4 (time of maximum level) (sec)
2. List T_3 (time aircraft is abeam) (sec)
3. Obtain $\delta T = T_4 - T_3$ (sec)
4. List V_j (aircraft TAS in Kt) (kt)
5. Obtain $\ell = 1.69 \cdot \delta T \cdot V_j$ (ft)
6. Obtain h_3 } Obtain from adjusted altimeter reading (ft)
7. Obtain h_4 } (ft)
8. Calculate $\gamma = \arcsin \frac{h_4 - h_3}{\ell}$ ($^\circ$)

- *9. Calculate $h = \sqrt{s^2 + h_3^2}$ (ft)
- *10. Obtain $\eta = \arctan \frac{h_3}{s}$ (°)
11. Calculate $c = 1116.9 \sqrt{\frac{273.2 + T (\text{°C})}{288.2}}$ (ft/sec)
12. Calculate $M = \frac{1.69 V_j}{c}$
13. Determine ξ from
- $$\xi = \arccos \left[\frac{s^2 + h_3^2 \tan^2 (90^\circ - \gamma) - h^2 - h_3^2 \csc^2 \gamma}{2h_3 \cdot h \cdot \csc \gamma} \right] \quad (^\circ)$$
14. Obtain $\gamma' = \xi - 90^\circ$ (°)
15. Calculate
- and
- $$A = \ell \cdot M + 2h \cdot \sin \gamma' \cdot M = M(\ell + 2h \sin \gamma')$$
- $$B = \left\{ \ell^2 + h^2 (1 - M^2) + 2h \ell \sin \gamma' + h^2 \sin^2 \gamma' M^2 \right\}^{\frac{1}{2}}$$
- *16. Obtain $z = \frac{-A + B}{(1 - M^2)}$ (ft)
17. Obtain $\Delta t' = \delta t - \frac{z}{c}$, and note sign (sec)
18. Calculate $\ell' = 1.69 V_j \Delta t'$, and note sign (ft)
19. Obtain θ from either:
- $$\theta = \arcsin \frac{h - \cos \gamma'}{z}$$
- $$\theta = \arccos \frac{\ell'^2 + z^2 - h^2}{2 \ell' z} \quad (^\circ)$$
- NOTE: If ℓ' is (-), $\theta > 90^\circ$
20. Calculate $h_3 = \frac{\ell'}{\ell} (h_4 - h_3) + h_3$ (δt)
21. Calculate $\alpha = \arcsin \frac{h_3}{z}$ (°)

CALCULATION STEPS FOR TAKEOFF POSITION (SEE FIGURE 3)

1. List T_1 (time aircraft is overhead) (sec)
2. List T_2 (time of maximum level) (sec)
3. Obtain $\delta T = T_2 - T_1$ (sec)

* In this and following pages, the * denotes calculated quantities important in determining the excess attenuation.

4. List 1.69 V_j (V_j is TAS in Kt) (Kt)
5. Obtain $\ell = 1.69 V_j \delta T$ (ft)
- *6. Obtain h } Obtain from photograph (ft)
7. Obtain h_2 } Obtain from flight data
- *8. Calculate $\gamma = \arcsin \frac{h_2 - h}{\ell}$ or (°)
 $\gamma = \arcsin \frac{h_{0M} - h}{(T_{0M} - T_1) 1.69 V_j}$
9. Calculate $c = 1116.9 \sqrt{\frac{273.2 + T(^{\circ}C)}{288.2}}$ (ft/sec)
10. Calculate $M = \frac{1.69 V_j}{c}$ and $(1-M^2)$
11. Calculate:

$$x = \frac{-(\ell \cdot M + 2h \sin \gamma \cdot M) + \sqrt{\ell^2 + h^2 (1-M^2) + 2h \ell \sin \gamma + h^2 \sin^2 \gamma M^2}}{(1 - M^2)}$$

NOTE: for $\gamma = 0$, (level flight)

$$x = \frac{-\ell \cdot M + \sqrt{\ell^2 + h^2 (1-M^2)}}{(1 - M^2)} \quad (\text{ft})$$

or $x = \frac{-A + B}{(1 - M^2)}$

where $A = \ell \cdot M + 2h \sin \gamma M$

$$B = \left\{ \ell^2 + h^2 (1 - M^2) + 2h \ell \sin \gamma + h^2 \sin^2 \gamma \cdot M^2 \right\}^{\frac{1}{2}}$$

12. Obtain $\Delta t' = \delta t - \frac{x}{C}$, and note sign of $\Delta t'$ (sec)
13. Calculate $\ell' = 1.69 V_j \cdot \Delta t'$ and note sign of ℓ' (ft)
14. Determine θ from either:

$$\theta = \arcsin \frac{h \cos \gamma}{x}$$

or $\theta = \arcsin \frac{\ell'^2 + x^2 - h^2}{2\ell' \cdot x}$

NOTE: if ℓ' is (-), $\theta > 90^\circ$

$$\text{and } \theta = \arcsin \frac{-h_1 \cos \gamma}{x}$$

CALCULATION STEPS FOR SPECTRUM ADJUSTMENTS AND COMPARISONS

1. Calculate speed adjustment

$$\Delta_1 = 10 \log \frac{V \text{ field}}{V \text{ ref.}}$$

2. Calculate torque or thrust adjustment Δ_2 from certification report charts or figures

3. Calculate distance adjustment

$$\Delta_3 = 20 \log \frac{h}{h_r}$$

4. For integrated spectrum adjustments to be applied to all frequency bands

$$\Delta_{IL} = \Delta_1 + \Delta_2 + \Delta_3$$

5. For composite spectrum adjustments to be applied to all frequency bands

$$\Delta_{ML} = \Delta_2 + \Delta_3 \quad (\text{from steps 2 \& 3})$$

6. Determine the IL-ML adjustment to be applied to the integrated spectrum levels at the reference distance. This adjustment is calculated for each frequency band from the linear regression line fitted to values of (IL-ML) versus log (distance).

7. Apply appropriate adjustments to the integrated spectra (steps 5 & 6) and to the composite spectra (step 4).

8. Adjust spectra for difference between field and reference temperature and humidity. Use actual and reference path distances at angle of maximum radiation, θ . Thus

$$\text{Reference distance} = \frac{h_r}{\sin \theta}$$

$$\begin{aligned} \text{Field distance} &= z \text{ for sideline position} \\ &= x \text{ for takeoff position} \end{aligned}$$

9. Compare adjusted sideline levels with adjusted levels for the takeoff position. Tabulate the differences per sideline position per flight. These differences represent the experimental excess attenuation referred to the overhead levels (position K in Figure 3).

REFERENCES

1. BBN Report 2757, "Hercules 382 FAR Part 36 Certification Program", September 1974
2. BBN Report 2603, "Learjet Models 24 and 25 FAR Part 36 Certification Program", January 1974
3. BBN Report 2935R, "Learjet Model 24D FAR Part 36 Certification Program", November 1975
4. BBN Report 4202, "NA 265-65 Sabreliner FAR Part 36 Noise Certification Program", September 1979
5. BMD Biomedical Computer Programs, Program BMD05R, 1967.